Pharmacological Research 165 (2021) 105463

Contents lists available at ScienceDirect

Pharmacological Research

journal homepage: www.elsevier.com/locate/yphrs

Properties of FDA-approved small molecule protein kinase inhibitors: A 2021 update

Robert Roskoski Jr.

Blue Ridge Institute for Medical Research, 3754 Brevard Road, Suite 116, Box 19 Horse Shoe, NC, 28742-8814, United States

ARTICLE INFO

Keywords:
Catalytic spine
Hydrophobic interaction
Protein kinase inhibitor classification
Protein kinase structure
Regulatory spine
Shell residues

Chemical compounds studied in this article:
Avapritinib (PubMED CID: 118023034)
Capmatinib (PubMED CID: 25145656)
Pemigatinib (PubMED CID: 86705659)
Pralsetinib (PubMED CID: 129073603)
Ripretinib (PubMED CID: 71584930)
Selpercatinib (PubMED CID: 134436906)
Selumetinib (PubMED CID: 10127622)
Tucatinib (PubMED CID: 51039094)
Upadacitinib (PubMED CID: 58557659)
Zanubrutinib (PubMED CID: 135565884)

ABSTRACT

Owing to the dysregulation of protein kinase activity in many diseases including cancer, the protein kinase enzyme family has become one of the most important drug targets in the 21st century. There are 62 FDA-approved therapeutic agents that target about two dozen different protein kinases and eight of these were approved in 2020. All of the FDA-approved drugs are orally effective with the exception of netarsudil (a ROCK1/2 non-receptor protein-serine/threonine kinase antagonist given as an eye drop for the treatment of glaucoma) and temsirolimus (an indirect mTOR inhibitor given intravenously for the treatment of renal cell carcinoma). Of the approved drugs, ten target protein-serine/threonine protein kinases, four are directed against dual specificity protein kinases (MEK1/2), thirteen block non-receptor protein-tyrosine kinases, and 35 target receptor protein-tyrosine kinases. The data indicate that 55 of these drugs are prescribed for the treatment of neoplasms (52 against solid tumors including breast, lung, and colon, nine against non-solid tumors such as leukemias, and four against both solid and non-solid tumors: acalabrutinib, ibrutinib, imatinib, and midostaurin). A total of three drugs (baricitinib, tofacitinib, upadacitinib) is used for the treatment of inflammatory diseases including rheumatoid arthritis. Seven of the approved drugs form covalent bonds with their target enzymes and are classified as TCIs (targeted covalent inhibitors). Of the 62 approved drugs, eighteen are used in the treatment of multiple diseases. Imatinib, for example, is approved for the treatment of eight different disorders. The most common drug targets of the approved pharmaceuticals include BCR-Abl, B-Raf, vascular endothelial growth factor receptors (VEGFR), epidermal growth factor receptors (EGFR), and ALK. The following eight drugs received FDA approval in 2020 for the treatment of the specified diseases: avapritinib and ripretinib (gastrointestinal stromal tumors), capmatinib (non-small cell lung cancer), pemigatinib (cholangiocarcinoma), pralsetinib and selpercatinib (non-small cell lung cancer, medullary thyroid cancer, differentiated thyroid cancer), selumetinib (neurofibromatosis type I), and tucatinib (HER2-positive breast cancer). All of the eight drugs approved in 2020 fulfill Lipinski's rule of five criteria for an orally effective medicine (MW of 500 Da or less, five or fewer hydrogen bond donors, 10 or fewer hydrogen bond acceptors, calculated $\log_{10}$ of the partition coefficient of five or less) with the exception of three drugs with a molecular weight greater that 500 Da: pralsetinib (534), selpercatinib (526) and ripretinib (510). This review summarizes the physicochemical properties of all 62 FDA-approved small molecule protein kinase inhibitors.

1. The importance of therapeutic protein kinase inhibitors

Because of overexpression and genetic alterations such as mutations and translocations, the dysregulation of protein kinase activity is involved in the pathogenesis of many diseases including autoimmune, cardiovascular, nervous, and inflammatory diseases as well as number of malignancies. Accordingly, this enzyme family has become one of the most important drug targets in the 21st century [1,2]. An estimated one-quarter of the drug discovery efforts in the world target protein kinases. The therapeutic success of imatinib in the treatment of

Abbreviations: AS, activation segment; BP, back pocket; C-spine, catalytic spine; CS1, catalytic spine residue 1; CL, catalytic loop; DMARDs, disease-modifying antirheumatic drugs; EGFR, epidermal growth factor receptor; F, front pocket; FGFR, fibroblast growth factor receptor; GIST, gastrointestinal stromal tumor; GK, gatekeeper; GRL, glycine-rich loop; HGF, hepatocyte growth factor; KLIFS-3, kinase-ligand interaction fingerprint and structure residue-3; LE, ligand efficiency; LipE, lipophilic efficiency; NSCLC, non-small cell lung cancer; PDGFR, platelet-derived growth factor receptor; PKA, protein kinase A; Ro5, Lipinski's rule of five; R-spine, regulatory spine; RS1, regulatory spine residue 1; Sh2, shell residue 2; VEGFR, vascular endothelial growth factor receptor.

E-mail address: rrj@brimr.org.

https://doi.org/10.1016/j.phrs.2021.105463
Received 22 January 2021; Accepted 22 January 2021
Available online 26 January 2021

Philadelphia chromosome-positive chronic myelogenous leukemias and its FDA approval in 2001 motivated the pursuit of orally effective protein kinase inhibitors [3]. This initial success resulted from the imatinib blockade of the activated chimeric BCR-Abl protein-tyrosine kinase, the chief biochemical defect that causes these leukemias.

The five thousand or more protein kinase structures in the public domain represent important aids in structure-based drug development. Furthermore, a larger number of proprietary structures exist within the pharmaceutical industry that are used in the drug development process. About 175 different orally effective protein kinase antagonists are in clinical trials worldwide [4]. A complete listing of these medicinals, which is regularly updated, can be found at www.icoa.fr/pkidb/. There are 62 FDA-approved therapeutic agents that target more than 20 different protein kinases (see supplementary material). Additional drugs targeting another two dozen protein kinases are in clinical trials worldwide [4,5]. However, these protein kinases represent only a small portion of the 518-member protein kinase enzyme family.

Manning et al. reported in a classical study that the human protein kinase lineage contains 478 typical and 40 atypical enzymes [6]. These enzymes catalyze the following generic reaction;

$$MgATP^{1-} + \text{protein–O:H} \rightarrow \text{protein–O:}PO_3^{2-} + MgADP + H^+$$

Based upon the nature of the phosphorylated −OH groups, these catalysts are divided into protein-tyrosine kinases (90 members), protein-tyrosine kinase–like enzymes (43), and protein-serine/threonine kinases (385). The protein-tyrosine kinase group includes both receptor (58) and non-receptor (32) entities. Furthermore, the kinase family includes a small cadre of catalysts such as MEK1/2 that catalyze the phosphorylation of both tyrosine and then threonine residues within the activation segment of their substrate protein kinases; MEK1/2 and related enzymes are classified as dual specificity protein kinases. About one in every 40 human genes encodes a protein kinase (518 protein kinase genes out of an estimated 20,000 human genes). Consequently, protein kinases constitute about 2.5 % of all human genes. Based upon a comprehensive analysis, Manning et al. found that 244 protein kinases map to cancer amplicons and disease loci [6]. Such analyses foreshadow a sizable increase in the number of protein kinases that will be pursued as targets for the treatment of many additional illnesses.

The US FDA has approved a total of 62 small molecule therapeutic protein kinase antagonists as of 1 January 2021 (see supplementary material), nearly all of which are orally effective with the exceptions of netarsudil (an eye drop) and temsirolimus (which is given intravenously). Of the 62 approved drugs, eleven target protein-serine/threonine protein kinases, three are directed against dual specificity protein kinases (MEK1/2), thirteen block non-receptor protein-tyrosine kinases, and 35 target receptor protein-tyrosine kinases (Table 1). The data indicate that 55 of these drugs are prescribed for the treatment of neoplasms (50 against solid tumors including those of breast, lung, and colon and eight against non-solid tumors such as leukemias, and three against both solid and non-solid tumors: acalabrutinib, ibrutinib, and imatinib). At least 25 of the approved medicinals are multikinase inhibitors. Because the specificity of many of these drugs has not been reported, it is likely that many more of these approved drugs are multikinase antagonists. Inhibiting multiple enzymes has potential advantages and disadvantages. On the one hand, the therapeutic effectiveness of multikinase inhibitors may be related to the inhibition of more than one target. For example, sunitinib and cabozantinib have potent off-target activity against Axl and this action may add to their clinical effectiveness [7]. On the other hand, the inhibition of off-target enzymes may contribute to adverse events or lead to various side effects. Accordingly, we have the dilemma of whether a magic shotgun is to be preferred over Paul Ehrlich's magic bullet (zauberkugel) [8].

Nine of the FDA-approved protein kinase inhibitors are used for the treatment of non-malignancies. For example, netarsudil is employed for the treatment of glaucoma, fedratinib is prescribed for the treatment of

Table 1
FDA-approved small molecule protein kinase inhibitors, their protein kinase targets, and therapeutic indications[c].

Drug (Code) Trade name	Year approved	Primary targets [a]	Therapeutic indications [b]
Abemaciclib (LY2835219) Verzenio	2017	CDK4/6	Combination therapy with an (i) aromatase inhibitor or with (ii) fulvestrant or as a monotherapy for breast cancers
Acalabrutinib (ACP-196) Calquence	2017	BTK	Mantle cell lymphomas, CLL, SLL
Afatinib (BIBW 2992) Tovok	2013	ErbB1/2/4	NSCLC
Alectinib (CH5424802) Alecensa	2015	ALK, RET	ALK-positive NSCLC
Avapritinib (BLU285) Ayvakit	2020	PDGFRα	GIST with *PDGFRα* exon 18 mutations
Axitinib (AG-013736) Inlyta	2012	VEGFR1/2/3	RCC
Baricitinib (LY 3009104) Olumiant	2018	JAK1/2	Rheumatoid arthritis
Binimetinib (MEK162) Mektovi	2018	MEK1/2	Combination therapy with encorafenib for $BRAF^{V600E/K}$ melanomas
Bosutinib (SKI-606) Bosulif	2012	BCR-Abl	CML
Brigatinib (AP 26113) Alunbrig	2017	ALK	ALK-positive NSCLC
Cabozantinib (BMS-907351) Cometriq	2012	RET, VEGFR2	Medullary thyroid cancers, RCC, HCC
Capmatinib (INC-280) Tabrecta	2020	c-MET	NSCLC with *MET* exon 14 skipping mutations
Ceritinib (LDK378) Zykadia	2014	ALK	ALK-positive NSCLC resistant to crizotinib
Cobimetinib (GDC-0973) Cotellic	2015	MEK1/2	$BRAF^{V600E/K}$ melanomas in combination with vemurafenib
Crizotinib (PF 2341066) Xalkori	2011	ALK, ROS1	ALK or ROS1-postive NSCLC
Dabrafenib (GSK2118436) Tafinlar	2013	B-Raf	$BRAF^{V600E/K}$ melanomas, $BRAF^{V600E}$ NSCLC, $BRAF^{V600E}$ anaplastic thyroid cancers
Dacomitinib (PF-00299804) Visimpro	2018	EGFR	*EGFR*-mutant NSCLC
Dasatinib (BMS-354825) Sprycell	2006	BCR-Abl	CML
Encorafenib (LGX818) Braftovi	2018	B-Raf	Combination therapy with binimetinib for $BRAF^{V600E/K}$ melanomas
Entrectinib (RXDX-101) Ignyta	2019	TRKA/B/C, ROS1	Solid tumors with NTRK fusion proteins, ROS1-positive NSCLC
Erdafitinib (JNJ-42756493) Balversa	2019	FGFR1/2/3/4	Urothelial bladder cancers
Erlotinib (OSI-774) Tarceva	2004	EGFR	NSCLC, pancreatic cancers
Everolimus (RAD001) Afinitor	2009	FKBP12/mTOR	HER2-negative breast cancers, pancreatic neuroendocrine tumors, RCC, angiomyolipomas, subependymal giant cell astrocytomas
Fedratinib (TG101348) Inrebic	2019	JAK2	Myelofibrosis
	2018	Syk	Chronic immune thrombocytopenia

(*continued on next page*)

Table 1 (*continued*)

Drug (Code) Trade name	Year approved	Primary targets [a]	Therapeutic indications [b]
Fostamatinib (R788) Tavalisse			
Gefitinib (ZD1839) Iressa	2003	EGFR	NSCLC
Gilteritinib (ASP2215) Xospata	2018	Flt3	AML
Ibrutinib (PCI-32765) Imbruvica	2013	BTK	CLL, mantle cell lymphomas, marginal zone lymphomas, graft vs. host disease
Imatinib (STI571) Gleevec	2001	BCR-Abl	Ph^+ CML or ALL, aggressive systemic mastocytosis, chronic eosinophilic leukemias, dermatofibrosarcoma protuberans, hypereosinophilic syndrome, GIST, myelodysplastic/ myeloproliferative disease
Lapatinib (GW572016) Tykerb	2007	EGFR, ErbB2/ HER2	HER2-positive breast cancers
Larotrectinib (LOXO-101) Vitrakvi	2018	TRKA/B/ C	Solid tumors with NTRK fusion proteins
Lenvatinib (AK175809) Lenvima	2015	VEGFR, RET	Differentiated thyroid cancers
Lorlatinib (PF-06463922) Lorbrena	2018	ALK	ALK-positive NSCLC
Midostaurin (CPG 41251) Rydapt	2017	Flt3	AML, mastocytosis, mast cell leukemias
Neratinib (HKI-272) Nerlynx	2017	ErbB2/ HER2	HER2-positive breast cancers
Netarsudil (AR11324) Rhopressa	2018	ROCK1/2	Glaucoma
Nilotinib (AMN107) Tasigna	2007	BCR-Abl	Ph^+ CML
Nintedanib (BIBF-1120) Vargatef	2014	FGFR1/2/ 3	Idiopathic pulmonary fibrosis
Osimertinib (AZD-9292) Tagrisso	2015	EGFR T970M	NSCLC
Palbociclib (PD-0332991) Ibrance	2015	CDK4/6	Estrogen receptor- and HER2-positive breast cancers
Pazopanib (GW786034) Votrient	2009	VEGFR1/ 2/3	RCC, soft tissue sarcomas
Pemigatinib (INCB054828) Pemazyre	2020	FGFR2	Advanced cholangiocarcinoma with a FGFR2 fusion or rearrangement
Pexidartinib (PLX3397) Turalio	2019	CSF1R	Tenosynovial giant cell tumors
Ponatinib (AP 24534) Iclusig	2012	BCR-Abl	Ph^+ CML or ALL
Pralsetinib (Blu-667) Gavreto	2020	RET	RET-fusion (i) NSCLC, (ii) medullary thyroid cancer, (iii) thyroid cancer
Regorafenib (GSK2118436) Tafinlar	2012	VEGFR1/ 2/3	Colorectal cancers
R406	2018	Syk	Chronic immune thrombocytopenia
Ribociclib (LEE011) Kisqali	2017	CDK4/6	Combination therapy with an aromatase inhibitor for breast cancers
Ripretinib (DCC-2618) Qinlock	2020	Kit, PDGFRα	Fourth-line treatment for GIST
Ruxolitinib (INCB-018424) Jakafi	2011	JAK1/2/ 3,Tyk	Myelofibrosis, polycythemia vera
	2020	RET	
Selpercatinib (CEGM9YBNG) Retevmo			RET fusion NSCLC and thyroid cancers and *RET* mutant medullary thyroid cancers
Selumetinib (AZD6224) Koselugo	2020	MEK1/2	Neurofibromatosis type I
Sirolimus (AY 22989) Rapamycin	1999	FKBP12/ mTOR	Kidney transplants, lymphangioleiomyomatosis
Sorafenib (BAY 43-9006) Nexavar	2005	VEGFR1/ 2/3	HCC, RCC, thyroid cancer (differentiated)
Sunitinib (SU11248) Sutent	2006	VEGFR2	GIST, pancreatic neuroendocrine tumors, RCC
Temsirolimus (CCI-779) Torisel	2007	FKBP12/ mTOR	RCC
Tofacitinib (CP-690550) Tasocitinib	2012	JAK3	Rheumatoid arthritis
Trametinib (GSK1120212) Mekinist	2013	MEK1/2	$BRAF^{V600E/K}$ melanomas, $BRAF^{V600E}$ NSCLC
Tucatinib (ONT-380) Tukysa	2020	ErbB2/ HER2	Combination second-line treatment for HER2-positive breast cancers
Upadacitinib (ABT-494) Rinvoq	2019	JAK1	Second-line treatment for rheumatoid arthritis
Vandetanib (ZD6474) Zactima	2011	VEGFR2	Medullary thyroid cancers
Vemurafenib (PLX-4032) Zelboraf	2011	B-Raf	$BRAF^{V600E}$ melanomas
Zanubrutinib (BGB3111) Brukinsa	2019	BTK	Mantle cell lymphomas

[a] Although many of these drugs are multikinase inhibitors, only the primary therapeutic targets are given here.

[b] ALL, acute lymphoblastic leukemias; AML, acute myelogenous leukemias; CLL, chronic lymphocytic leukemias; CML, chronic myelogenous leukemias; ErbB2/HER2, human epidermal growth factor receptor-2; GIST, gastrointestinal stromal tumors; HCC, hepatocellular carcinomas; NSCLC, non-small cell lung cancers; Ph^+, Philadelphia chromosome positive; RCC, renal cell carcinomas; SLL, small lymphocytic leukemias.

[c] Drugs not previously reviewed in Refs. [9,10] are given in **bold** type.

myelofibrosis, nintedanib is used for the treatment of idiopathic pulmonary fibrosis, sirolimus is exploited for the treatment of renal graft vs. host disease, fostamatinib is prescribed for the treatment of chronic immune thrombocytopenia, ruxolitinib is used for the treatment of myelofibrosis and polycythemia vera, baricitinib and upadacitinib are employed for the treatment of rheumatoid arthritis, and tofacitinib is used for the treatment of rheumatoid arthritis, Crohn disease, and ulcerative colitis [9,10]. Moreover, sirolimus and ibrutinib are prescribed for the treatment of both malignant and non-malignant diseases.

Seven drugs form covalent bonds with their target enzymes and are classified as TCIs (targeted covalent inhibitors) [11]. These include acalabrutinib (inhibiting BTK in mantle cell lymphomas), ibrutinib (inhibiting BTK in chronic lymphocytic leukemias, mantle cell lymphomas, marginal zone lymphomas, chronic graft vs. host disease, and Waldenström macroglobulinemia), zanubrutinib (targeting BTK in mantle cell lymphomas), neratinib (targeting ErbB2 in HER2-positive breast cancers), osimertinib (targeting *EGFR T970M* mutants in NSCLC), afatinib (targeting EGFR in NSCLC), and dacomitinib (inhibiting mutant *EGFR* in lung cancers). The closely related *EGFR* and *ErbB4* of the epidermal growth factor receptor family consisting of ErbB1/2/3/4

are the most frequently mutated protein kinases in all cancers [3]. For a summary of the properties of small molecule protein kinase inhibitors that were approved by the FDA prior to 2020, see Refs. [9,10].

Of the 62 FDA-approved small molecule protein kinase antagonists, nineteen are used in the treatment of multiple diseases. Imatinib, for example, is used in the treatment of eight distinct disorders (Table 1). This medicinal inhibits Abl (and the BCR-Abl chimera – responsible for the pathogenesis of chronic myelogenous leukemias), Abl2, Kit (the stem cell factor receptor), PDGFRα/β, epithelial discoidin domain-containing receptor-1 (DDR1) and receptor-2 (DDR2). The latter two enzymes are activated by collagen and they participate in cell proliferation, migration, differentiation, and remodeling the extracellular matrix. Imatinib is FDA-approved for (i) the first-line treatment of Philadelphia chromosome-positive chronic myelogenous leukemias, (ii) dermatofibrosarcoma protuberans, (iii) *KIT* mutation-positive gastrointestinal stromal tumors, (iv) chronic eosinophilic leukemias, (v) hypereosinophilic syndrome, (vi) myelodysplastic/myeloproliferative diseases with *PDGFR* gene-rearrangements, and (vii) as a second-line treatment for aggressive systemic mastocytosis without the *KIT* ^{D816V} mutation and (viii) acute lymphoblastic leukemias [9]. Imatinib is used off-label for the treatment of chordomas, chronic myelogenous leukemias following allogeneic stem cell transplantations, desmoid tumors, and advanced *KIT*-mutant melanomas. Imatinib is thus a broad-spectrum inhibitor.

2. Protein kinase structure and mechanism

2.1. Primary, secondary, and tertiary structures

The newly approved drugs described in this review interact with (at least) nine different protein kinases so that the following description is all encompassing. As initially described by Knighton et al. for PKA (protein kinase A), protein kinases possess a small amino-terminal lobe and large carboxyterminal lobe [12]. The small lobe consists of a five-stranded antiparallel β-sheet (β1–β5) structure and an αC-helix that occurs in active or dormant orientations [13,14]. The amino-terminal lobe also contains a conserved glycine-rich (GxGxΦG) loop, sometimes called the P-loop (for phosphate), which links the β1- and β2-strands; the Φ denotes a hydrophobic residue. Moreover, a conserved valine residue follows the glycine-rich loop (GxGxΦGxV) and this valine makes hydrophobic contact with the adenine moiety of ATP as well as several small molecule protein kinase antagonists. Protein kinases contain a conserved AxK signature sequence within the β3-strand and a conserved glutamate near the middle of the αC-helix. A salt bridge occurs between the β3-strand lysine (K) and the αC-helix glutamate (E) in catalytically active protein kinases and this structure corresponds to the "αC_{in}" conformation (Fig. 1A). The αC_{in} conformation is necessary, but not sufficient, for the expression of full enzyme activity. Moreover, the absence of this salt bridge indicates that the enzyme lacks activity and the resulting structure corresponds to the "αC_{out}" conformation (Fig. 1E). The transformation of the αC_{out} conformation to the αC_{in} structure is required for catalytic activity.

The large lobe is predominantly α-helical with eight conserved helices (αD–αI, αEF1, αEF2) (Fig. 1A) [15]. The large lobe of active protein kinases also contains four short β-strands (β6–β9). The second residue of the β7-strand, which occurs on the floor of the adenine binding pocket, makes hydrophobic contact with all known ATP-competitive protein kinase antagonists. The carboxyterminal lobe contains a catalytic loop that assists in the transfer of the γ-phosphoryl group from ATP to the protein substrates. The C-terminal lobe also positions the protein/peptide substrate to enable catalysis.

Hanks and Hunter described a dozen subdomains (I–VIa, VIb–XI) that make up the operational core of protein kinases [16]. The K/E/D/D (Lys/Glu/Asp/Asp) signature plays a vital role in the catalytic activity of essentially all protein kinases. The *K* of *K*/E/D/D is the β3-strand lysine residue that forms salt bridges with (i) the αC-glutamate to form the αC_{in} structure as well as (ii) the α-phosphate of ATP as depicted for EGFR (Fig. 2). A proline residue within the activation segment (P877)

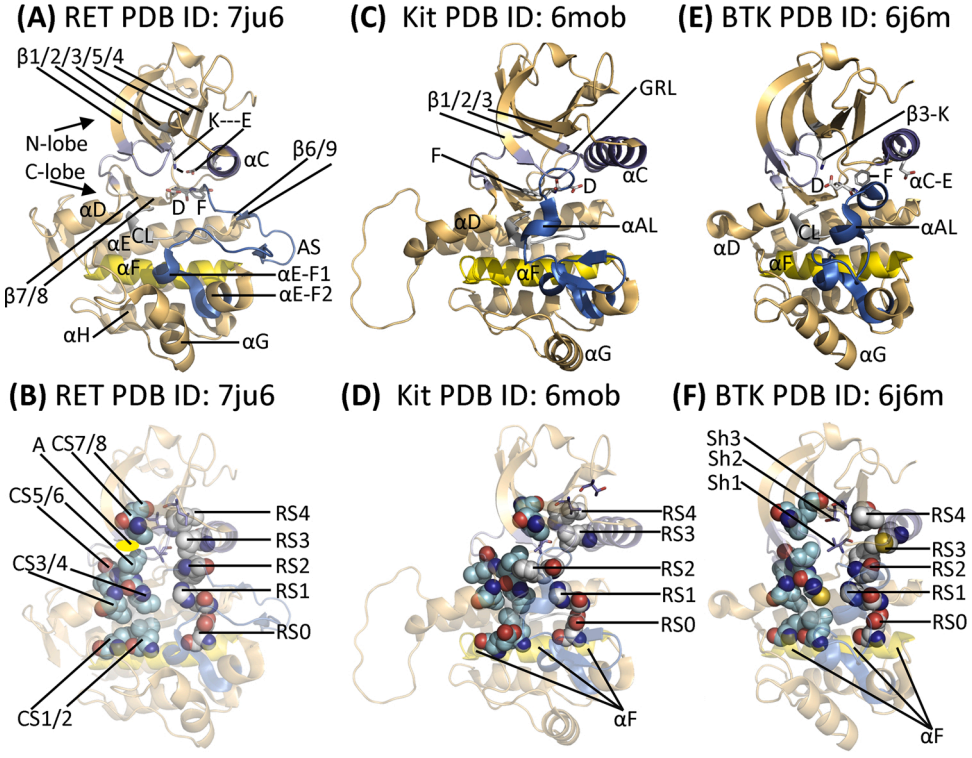

Fig. 1. (A) Active RET and its spine residues (B). (C) DFG-D_{out} inactive Kit and its spine residues (D). (E) αC_{out} inactive BTK and its spine residues (F). A, adenine; AL, activation loop; AS, activation segment; D, aspartate; F, phenylalanine. Figs. 1–4C, 7 and 8 were prepared using the PyMOL Molecular Graphics System Version 1.5.0.4 Schrödinger, LLC.

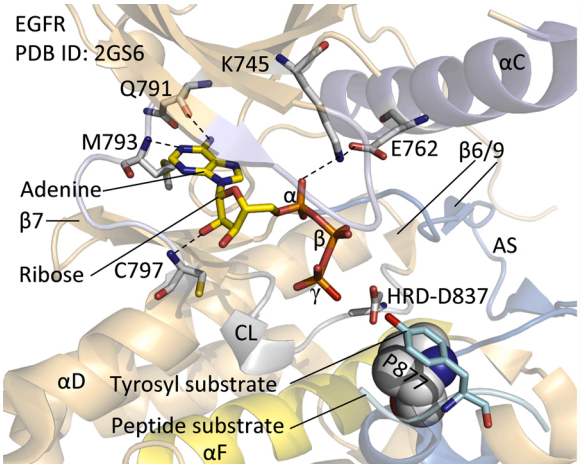

Fig. 2. ATP-binding site of active EGFR. AS, activation segment; P877, proline 877.

positions the tyrosyl substrate residue. Moreover, the catalytic-loop HRD-aspartate (the first *D* of K/E/*D*/D), which is a Lowry-Brönsted base (proton acceptor), plays a vital role during catalysis. Madhusudan et al. suggested that the catalytic-loop HRD-aspartate removes the proton from the protein substrate −OH group and this process promotes the nucleophilic attack of oxygen with the γ-phosphorus atom of ATP (Fig. 3) [17]. Additionally, Zhou and Adams postulated that the catalytic-loop HRD-aspartate positions the hydroxyl group of the protein substrate in a position that aids the in-line nucleophilic attack [18]. See Ref [19]. for a general overview of protein kinase enzymology and Table 2 for a list of the important residues in the protein kinase targets of the 10 protein kinase antagonists not previously covered in this review series [9,10] (with EGFR/ErbB1 serving as a surrogate for ErbB2/HER2).

The second *D* of the K/E/D/*D* canonical signature signifies the first residue of the protein substrate binding activation segment. The activation segment of all protein kinases begins with DFG and nearly all activation segments end with APE. The activation segment, which is about 35–40 residues long, is a key structural and regulatory element in all protein kinases [20]. The amino acid sequence of the catalytic loop of protein kinases is HRD(x)$_4$N. The primary structure of the activation

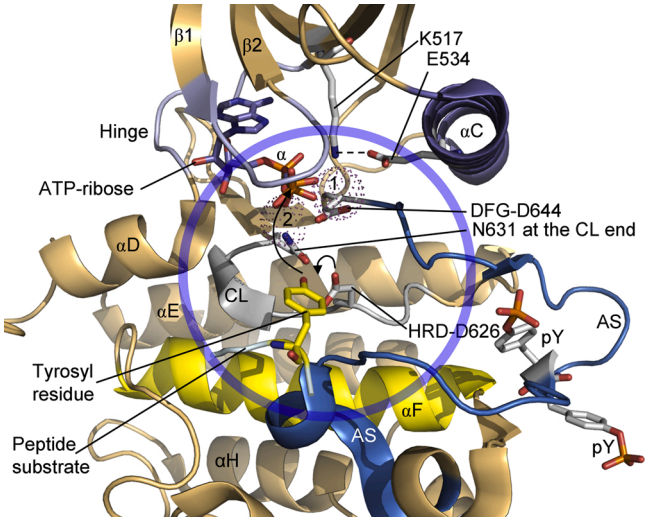

Fig. 3. Mechanism of the FGFR2 protein kinase reaction (PDB ID: 2pvf). The chemistry occurs within the colored circle. AS, activation segment; CL, catalytic loop; pY, phosphotyrosine. Mg^{2+}(1) and Mg^{2+}(2) are depicted as the dots labeled 1 and 2.

Table 2
Important residues in selected human protein kinases.

	BTK	EGFR	FGFR2	JAK1	Kit	MEK1	MET	PDGFRα	RET
Number of residues	659	1210	821	1154	976	393	1390	1089	1114
Signal peptide	None	1–24	1–21	None	1–25	None	1–24	1–23	1–28
Extracellular segment	None	25–645	22–377	None	26–524	None	25–932	24–528	29–635
Transmembrane segment	None	646–668	378–398	None	525–545	None	933–955	529–549	636–657
Intracellular portion	1–659	669–1210	399–821	1–1154	546–976	None	956–1390	550–1089	658–1114
Protein kinase domain	402–655	712–979	481–770	875–1153	589–937	68–361	1078–1345	593–954	724–1016
Glycine-rich loop	^{409}GTGQFG^{414}	^{719}GSGAFG^{724}	^{488}GEGCFG^{493}	^{882}GEGHFG^{887}	^{596}GAGAFG^{601}	^{75}GAGNGG^{80}	^{1085}GRGHFG^{1090}	^{600}GSGAFG^{605}	^{731}GEGEFG^{736}
The β3-*K* of *K*/E/D/D	K430	K745	K517	K908	K623	K97	1110	K627	K758
αC-*E* of K/*E*/D/D	E445	E762	E534	E925	E640	E114	1127	E644	E775
Hinge residues	^{475}EYM^{477}	^{791}QLM^{793}	^{565}EYA^{567}	^{957}EFL^{959}	^{671}EYC^{673}	^{144}EHM^{146}	^{1158}PYM^{1160}	^{675}EYC^{677}	^{805}EYA^{807}
Gatekeeper residue	T474	T790	V564	M596	T670	M143	L1157	T674	V804
Catalytic HR*D* residue, the first *D* of K/E/*D*/D	D521	D837	D626	D1003	D792	D190	D1204	D818	D874
Catalytic loop *N* (HRD(x)$_4$*N*	N526	N842	N631	N1008	N797	N195	N1209	N823	N879
AS[a] *DFG*, the second *D* of K/E/*D*/*D*	D539	D855	D644	D1021	D810	D208	D1222	D836	D892
AS[a] tyrosine phosphorylation site	Y551	Y869	Y656/7	Y1034/5	Y703, Y721, Y730	S218, S222	Y1230, Y1234/5	Y849	Y900/905
End of the AS[a]	^{565}PPE^{567}	^{882}ALE^{884}	^{671}APE^{673}	^{1049}APE^{1051}	^{837}APE^{839}	^{231}SPE^{233}	^{1251}ALE^{1253}	^{863}APE^{865}	^{919}AIE^{921}
Molecular weight (kDa)	76.3	134	92.0	133.3	110	43.4	155.5	122.6	124.3
UniProtKB ID	Q06187	P00533	P21802	P23458	P10721	Q02750	P08581	P16234	P07949

segment occurs after the catalytic loop. Two Mg^{2+} ions, which are designated as Mg^{2+}(1) and Mg^{2+}(2), are required for the catalytic activity of almost all protein kinases (Fig. 3).

In terms of length and primary structure, the middle of the activation segment varies greatly among all of the members of the protein kinase superfamily [1]. The activation segment of nearly all protein kinases contains one or more phosphorylatable residues. Furthermore, activation segment phosphorylation is required for the expression of full enzyme activity in most, but not all, protein kinases. ErbB1/2/4 of the EGFR family, for example, exhibit full catalytic activity without activation segment phosphorylation. The initial part (DFG) of the activation segment occurs spatially near the conserved HRD sequence of the catalytic loop and the N-terminus of the αC-helix. Although the αC-helix occurs within the small lobe, it occupies a strategically important position between both lobes.

The activation segment of protein kinases exhibits an open or extended structure in all active protein kinases (Fig. 1A) and a closed configuration in most inactive kinases (Fig. 1C) [1]. The first two residues of the activation segment occur in two different conformations. The DFG-D side chain of active and functional protein kinases points toward the ATP-binding site and it coordinates Mg^{2+}(1). This structure is called the "DFG-D_{in}" conformation (Fig. 1A). In the inactive activation segment conformation that is seen in many protein kinases, the DFG-D points away from the ATP-binding site. This structure is called the "DFG-D_{out}" conformation (Fig. 1C). It is the ability of DFG-*D* to bind (DFG-D_{in}) or not bind (DFG-D_{out}) Mg^{2+}(1) within the active site that is essential. See Ref. [1] for more information about these two activation segment arrangements.

2.2. Protein kinase hydrophobic skeletons

Kornev et al. examined the tertiary structures of active and dormant configurations of about 24 protein kinases to identify functionally and structurally critical residues [21,22]. Their analyses revealed a combination of eight amino acid residues that make up a catalytic spine (C-spine) and four amino acid residues that make up a regulatory spine (R-spine). Residues that make up these spines are derived from both the small and large lobes. The catalytic and regulatory spines generate a stable, but flexible, ensemble that is catalytically active. The R-spine positions the protein substrate and the C-spine positions ATP for catalysis. The R-spine contains residues from both the activation segment and the αC-helix, whose structures are important in determining active and inactive enzyme states. The precise positioning and alignment of both spines are necessary, but not sufficient, for the formation of catalytically competent protein kinases.

The R-spine consists of the first residue of the β4-strand and an amino acid four residues N-terminal to the conserved αC-glutamate within the αC-helix, which are within the small lobe [21]. This spine also contains the catalytic loop HRD-histidine and the activation segment DFG-phenylalanine within the large lobe. The HRD-histidine backbone NH— group hydrogen bonds with the side chain of a conserved aspartate within the αF-helix. From the bottom to the top of the structure, Meharena et al. designated the R-spine residues as RS0, RS1, RS2, RS3, and RS4 [23]. We later called the catalytic spine residues from the bottom to the top as residues CS1–8 (Fig. 1B and D) [24]. The C- and R-spine residues and the shell residues of the nine protein kinases considered in this review are listed in Table 3.

The protein kinase spine and shell residues play a crucial role in the structure and activity of protein kinases; it is not possible to overemphasize their importance in the functioning of the protein kinase superfamily as well as their interactions with small molecule kinase inhibitors. For a summary of the properties of the spine and shell residues and their interactions with small molecule inhibitors of selected members of the protein kinase super family, see the following reviews: Refs. [25–27] for the ALK pleotrophin and midkine receptor protein-tyrosine kinase, Refs. [28–30] for the EGFR family of protein-tyrosine kinases, Ref. [31] for the fibroblast growth factor receptor family of protein-tyrosine kinases, Ref. [32] for the Kit stem cell receptor protein-tyrosine kinase, Ref. [33] for the PDGFRα/β protein-tyrosine kinases, Ref. [34] for the RET glial-cell derived receptor protein-tyrosine kinase, Ref. [35] for the VEGFR1/2/3 protein-tyrosine kinases, Ref. [36] for the ROS1 orphan receptor protein-tyrosine kinase, Refs. [11,37] for the Bruton non-receptor protein-tyrosine kinase, Refs. [38,39] for the Src non-receptor protein-tyrosine kinase, Ref. [40] for the Janus non-receptor protein-tyrosine kinase, Ref. [41] for the MEK1/2 dual specificity protein kinases, Refs. [42,43] for the ERK1/2 protein-serine/threonine kinases, Refs. [15,44] for the cyclin-dependent protein-serine/threonine kinase family, and Refs. [45,46] for the Raf protein-serine/threonine kinases.

Protein kinase catalytic spines consist of two residues from the amino-terminal lobe and six residues from the carboxyterminal lobe. The adenine base of ATP couples these two parts of the C-spine together and this interaction facilitates the closure of the two lobes of the enzyme [22]. The completion of the C-spine by binding ATP readies the enzyme

Table 3
Spine and shell residues in selected human protein kinases.

	Symbol	KLIFS No.[a]	BTK	EGFR	FGFR2	JAK1	Kit	MEK1	MET	PDGFRα	RET
Regulatory spine											
β4-strand (N-lobe)	RS4	38	L460	L777	L550	Y940	L656	F129	L1157	L660	L790
C-helix (N-lobe)	RS3	28	M449	M766	M538	L929	L644	L118	M1131	M648	L779
Activation loop F of DFG (C-lobe)	RS2	82	F540	F856	F645	F1022	F811	F209	F1223	F837	F893
Catalytic loop His (C-lobe)	RS1	68	H519	H835	H624	H1001	H790	H188	H1202	H816	H872
F-helix (C-lobe)	RS0	None	D579	D896	D685	D1063	D851	D245	D1254	D877	D933
R-shell											
Two residues upstream from the gatekeeper	Sh3	43	I472	L788	V562	L954	V668	I141	V1155	I672	L802
Gatekeeper, end of β5-strand	Sh2	45	T474	T790	V564	M956	T670	M143	L1157	T674	V804
αC-β4 loop	Sh1	36	V458	C775	I548	V938	V654	V127	L1140	V658	I788
Catalytic spine											
β3-AxK motif (N-lobe)	CS8	15	A428	A743	A515	A906	A621	A95	A1108	A625	A756
β2-strand (N-lobe)	CS7	11	V416	V726	V495	V889	V603	V82	V1092	V607	V738
β7-strand (C-lobe)	CS6	77	L528	L844	L633	L1010	L799	L197	M1211	L825	L881
β7-strand (C-lobe)	CS5	78	V529	V845	V634	V1011	L800	V198	L1212	L826	V822
β7-strand (C-lobe)	CS4	76	C527	V843	V632	V1009	I798	I196	C1210	V824	I880
D-helix (C-lobe)	CS3	53	L482	L798	L572	L964	L678	L151	L1165	L682	L812
F-helix (C-lobe)	CS2	None	I590	L907	I696	L1074	L862	M256	L1276	I888	I944
F-helix (C-lobe)	CS1	None	L586	T903	L692	T1070	F858	S252	L1272	L884	L940

[a] klifs.net.

for catalysis. The two small lobe residues that bind to the adenine base of ATP include the conserved β2-strand valine (CS7) following the glycine-rich loop and the conserved β3-strand alanine (CS8) from the AxK motif. Moreover, a hydrophobic CS6 from the middle of the β7-strand of the large lobe interacts with the adenine base of ATP. CS4 and CS5 interact hydrophobically with CS3 at the beginning of the αD-helix. Furthermore, CS3 makes hydrophobic contact with the neighboring CS4 and CS1 within the αF-helix below it. Both the catalytic and regulatory spines are supported by the hydrophobic αF-helix below them, which serves as a major buttress for the assembly and stabilization of the entire protein kinase domain. The protein kinase hinge and linker residues connect the small and large lobes of protein kinases and the 6-amino group of ATP forms a hydrogen bond with the carbonyl group of the first hinge residue. Additionally, the *N*1 of the adenine base of ATP forms a hydrogen bond with the backbone amide group of the third hinge residue. Nearly all small-molecule steady-state ATP competitive protein kinases inhibitors form hydrogen bonds with the backbone residues of the hinge, most commonly with the third hinge residue [24].

Based upon the results of site-directed mutagenesis experiments, Meharena et al. discovered three residues in murine PKA that strengthen the regulatory spine, which they designated as shell residues (Sh1, Sh2, and Sh3) [23]. While the V104G Sh1 mutant had 5% of the catalytic activity of wild type PKA, their M120G/M118G Sh2/Sh3 double mutant completely lacked catalytic activity. These findings showed that the shell residues enable PKA activity. One infers that shell residues play a similar activating and stabilizing role in all protein kinases. The Sh1 residue occurs within the loop connecting the αC-helix and the β4-strand, the so-called back loop. The Sh2 or gatekeeper residue occurs immediately before the hinge region at the end of the β5-strand and the Sh3 residue occurs two residues upstream from the Sh2 residue within the β5-strand (Fig. 1F).

The gatekeeper label signifies the role that this residue plays in controlling access to the hydrophobic pocket adjacent to the adenine binding pocket [47,48] that is often occupied by structural elements of many small molecule protein kinase antagonists. Based upon the results of Meharena et al. [23], only three of the 14 amino acids close to RS3 and RS4 in PKA are conserved. To reiterate, many small molecule therapeutic steady-state ATP-competitive protein kinase blockers interact with the R-spine (RS2/3), the C-spine (CS6/7/8), and shell (Sh1 and Sh2) residues. Ung et al. reported that about 75 % of protein kinases have a relatively large gatekeeper residue (e.g., Phe, Leu, Met) while about 25 % have smaller gatekeeper residues (e.g., Val, Thr) [49]. Also of importance, the gatekeeper residue is also one of the more common sites of drug resistance mutations [3,50]

3. Protein kinase-inhibitor classification and inhibitor-binding pockets

Based upon the work of others [48,51–53], we divided the small molecule protein kinase inhibitors into seven main groups including reversible (Groups I, I½, II, III, IV, and V) and irreversible inhibitors (VI) as described in Table 4. We divided the type I½ and type II inhibitors into A and B subtypes [24]. Type A drugs are compounds that extend past the gatekeeper residue into the back cleft. In contrast, type B drugs are compounds that do not extend into the back cleft. The potential importance of this difference, based on preliminary data, is that type A inhibitors bind with longer residence times to their protein target as compared with type B inhibitors [24]. Sorafenib is a type IIA VEGFR antagonist and sunitinib is a type IIB VEGFR inhibitor, both of which are FDA-approved for the treatment of renal cell carcinomas. The type IIA antagonist has a residence time greater than 64 min while that of the type IIB inhibitor has a residence time of less than 2.9 min [24].

We followed the lead of Liao [54], van Linden et al. [55], and Kanev et al. [56] in describing and characterizing drug-binding pockets. A general overview depicting the location of the pockets and subpockets is depicted in Fig. 4 and the location of important residues nearby various pockets is described in Table 5. The region between the protein kinase small and large lobes is divided into a front pocket or front cleft, a gate area, and a back cleft. The back pocket or hydrophobic pocket II (HPII) includes the gate area and the adjoining back cleft. The front cleft includes the glycine-rich loop, the adenine-binding pocket, the hinge residues, the linker residues that connect the hinge residues to the C-terminal lobe αD-helix, and the catalytic loop (HRD(x)$_4$N).

Table 4
Classification of small molecule protein kinase inhibitors[a].

Inhibitor type	Properties
I	Binds in and around the ATP-binding pocket of an active enzyme
I½ A/B	Binds in and around the ATP-binding pocket of an inactive DFG-D_{in} enzyme
I½ A	Extends into the back cleft
I½ B	Does not extend into the back cleft
II A/B	Bind in and around the ATP-binding site of an inactive DFG-D_{out} enzyme
II A	Extends into the back cleft
II B	Does not extend into the back cleft
III	Allosteric inhibitor bound next to the ATP-binding site
IV	Allosteric inhibitor bound away from the ATP-binding site
V	Bivalent inhibitor spanning two kinase domain regions
VI	Covalent inhibitor

[a] Adapted from Ref. [24].

Type I inhibitors characteristically bind within the front cleft. The gate area consists of residues from both the small and large lobes. The gate includes the final three residues of the β3-strand and the first two residues of the β3-αC loop. The gate area also includes the residue immediately before the activation segment (the x of xDFG) and the first four residues of the activation segment. The back cleft contains the central portion of the αC-helix, the β4-strand, the last two residues of the β5-strand. It also contains the first two and fifth residues from the αE-helix and the two residues preceding the catalytic loop HRD (Fig. 4C). Many type I½ inhibitors occupy both the front cleft and a portion of the back cleft. One of the overall goals in the design and development of small molecule protein kinase blockers is to achieve selectivity and thereby reduce off-target side effects [52]; this procedure can be assisted by comparing drug interactions with target and non-target enzymes [5,57–59]. Designing pharmacophore attachments that bind to residues lining the various pockets and sub-pockets within the cleft plays a tactical role in protein kinase inhibitor drug discovery and development with the goal of maximizing drug affinity.

van Linden et al. and Kanev et al. formulated a comprehensive catalogue describing drug and ligand binding to more than 5200 human and mouse protein kinase domains [55,56]. Their KLIFS (kinase–ligand interaction fingerprint and structure) catalogue includes an alignment of 85 ligand binding-site residues occurring in both the small and large lobes; this guide facilitates the classification of drugs and ligands depending upon their binding properties. This information assists in the detection of common and unique drug-enzyme interactions. Moreover, these authors devised a standard amino acid residue numbering system that aids in the comparison of different protein kinase targets. Table 3 describes the relationship of the KLIFS database nomenclature and the catalytic spine, shell, and regulatory spine amino acid residue numbering system and Fig. 5 illustrates the location of the KLIFS residues within the protein kinase domain. Moreover, these investigators launched a helpful free and searchable web site that is periodically updated and it provides complete data on the interaction of protein kinases with drugs and ligands (klifs.net).

Moreover, Carles et al. created a comprehensive listing of protein kinase inhibitors that have been approved or that are in clinical trials [4]. They produced a free and searchable web site that is updated regularly and provides the structure of the various inhibitors, their target protein kinases, therapeutic indications, physical properties, the year of first approval (if applicable), and their trade name (http://www.

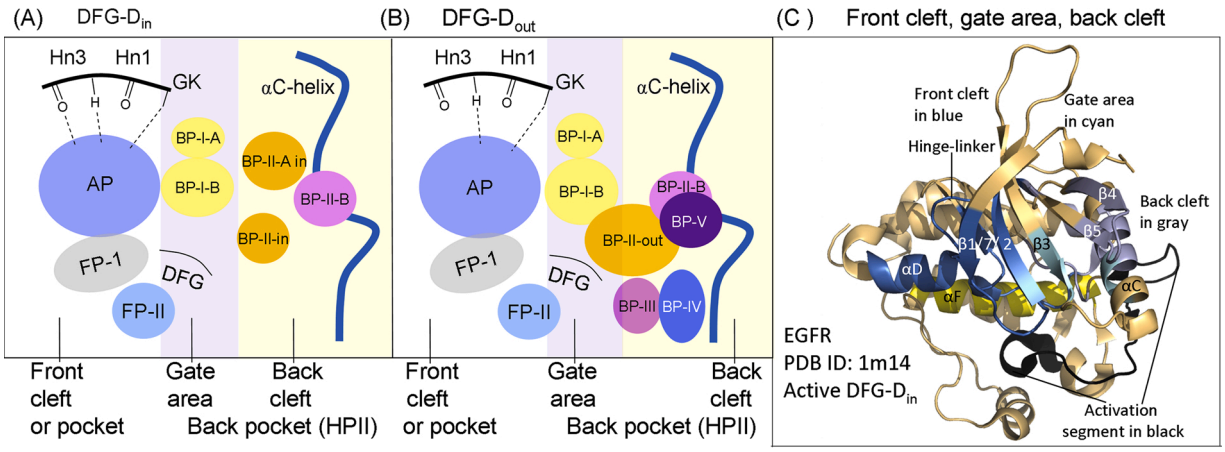

Fig. 4. (A) Location of the protein kinase domain drug-binding pockets in the DFG-D$_{in}$ enzyme form. (B) Location of the drug-binding pockets in the DFG-D$_{out}$ enzyme form. Adapted from Refs. [54–56]. (C) Location of the protein kinase front cleft, gate area, and back cleft. AP, adenine pocket; BP, back pocket; FP, front pocket; Hn, hinge; HPII, hydrophobic pocket II; GK, gatekeeper.

Table 5
Location of important residues within the front cleft, gate area, and back cleft.

Description	Location	KLIFS residue no.[a]
GxGxΦG	Front cleft	4–9
β2-strand V (CS7)	Front cleft	11
β3-strand A (CS8)	Front cleft	15
HRD with DFG-D$_{in}$	Front cleft	68–70
HRD(x)$_4$N-N	Front cleft	75
β7-strand CS6	Front cleft	77
β3-strand K; three residues before the αC-helix	Gate area	17
αC-β4 penultimate back loop residue	Gate area	36
Gatekeeper	Gate area	45
The x of xDFG	Gate area	80
DFG	Gate area	81–83
αC-helix E	Back cleft	24
RS3	Back cleft	28
HRD with DFG-D$_{out}$	Back cleft	68–70

[a] Ref. [55,56].

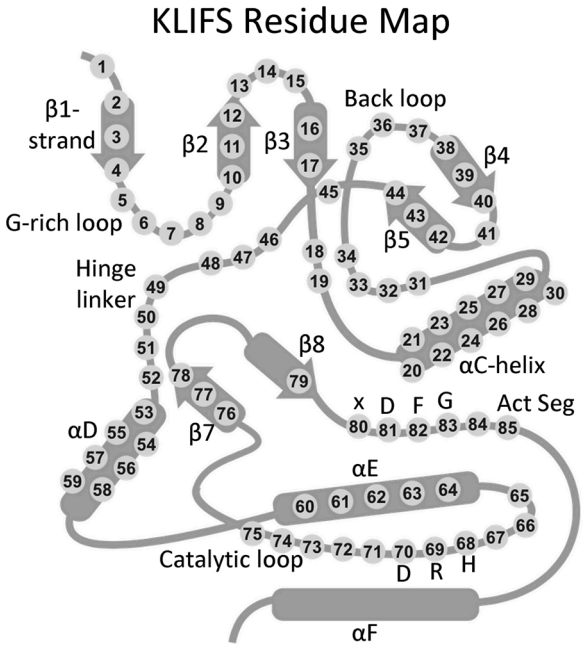

Fig. 5. The location of the KLIFS residues within a generic protein kinase domain. Act Seg, activation segment.

icoa.fr/pkidb/). Similarly, the Blue Ridge Institute for Medical Research maintains a web site that lists the FDA-approved protein kinase inhibitors and presents their (i) structures, (ii) number of hydrogen bond donors/acceptors, (iii) calculated log$_{10}$ of the distribution coefficient, (iv) number of rings and rotatable bonds, (v) year of initial approval, (vi) primary protein kinase targets, (vii) and clinical indications. The site also provides a link to the corresponding FDA labels. This web site, which is found at www.brimr.org/PKI/PKIs.htm, is regularly updated.

4. Drug-enzyme interactions

Pralsetinib is a pyrazolo-pyrimidine derivative (Fig. 6A) that is FDA-approved for the treatment of NSCLC, medullary thyroid cancers, and differentiated thyroid cancers bearing RET-fusion proteins [60]. RET (rearranged during transfection) mediates signaling related to cell growth and differentiation [34]. Its ligands include GDNF (glial-cell derived neurotrophic factor), NTRN (neurturin), ARTN (artemin), and PSPN (persephin). RET fusion proteins are found in 10–20 % of papillary thyroid cancers and 1–2 % of NSCLC patients [60]. Moreover, RET point mutations are found in 60–90 % of advanced medullary thyroid cancers. Cabozantinib and vandetanib were previously used in the treatment of RET-driven diseases, but off target toxicities and inadequate inhibition of RET limited their usefulness in these disorders.

The X-ray crystal structure of pralsetinib bound to RET [61] shows that the amino group of the compound forms a hydrogen bond with the carbonyl group of the third hinge residue (A807) and the nitrogen atoms of the pyrazolo group form hydrogen bonds with the N—H moiety of A807 and the carbonyl group of E805 (the first hinge residue) (Fig. 7A). The drug makes hydrophobic contact with the Sh2 gatekeeper residue, three spine residues (CS6/7/8), and L730 (the KLIFS-3 residue). The compound also interacts hydrophobically with G731, E732, G733, G736 of the G-rich loop, K737 of the β2-strand, AxK-K758, M759 and L760 of the β3-strand, L772 of the αC-helix, and ^{806}YAKYGS^{811} of the hinge-linker segment. The drug binds to the front pocket and the FP—II subpocket of an active enzyme form and is thus classified as a type I inhibitor [24]. See Refs. [62,63] for a review of the properties of pralsetinib that led to its FDA-approval.

Selpercatinib is a pyrazolo[1,5*a*]pyridine derivative (Fig. 6B) that is also FDA-approved for the treatment of NSCLC, medullary thyroid cancers, and differentiated thyroid cancers bearing RET-fusion proteins [60]. The X-ray crystal structure of this compound bound to RET shows that a pyrazolo nitrogen from the drug forms a hydrogen bond with the N—H group of A807 (Fig. 7B). The drug makes hydrophobic contact with the Sh2 gatekeeper residue, three spine residues (CS6/7/8), and L730 (the KLIFS-3 residue). The compound also interacts

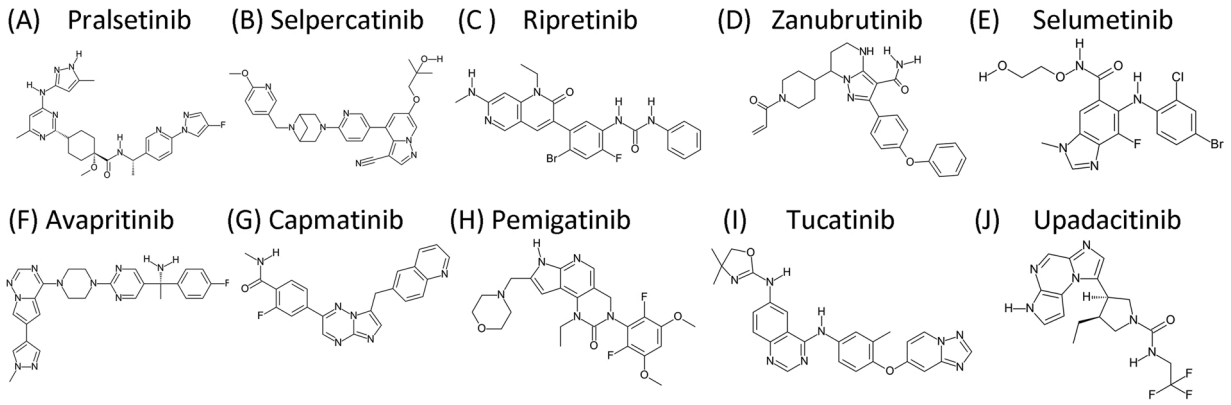

Fig. 6. (A-J). Chemical structures of selected protein kinase inhibitors.

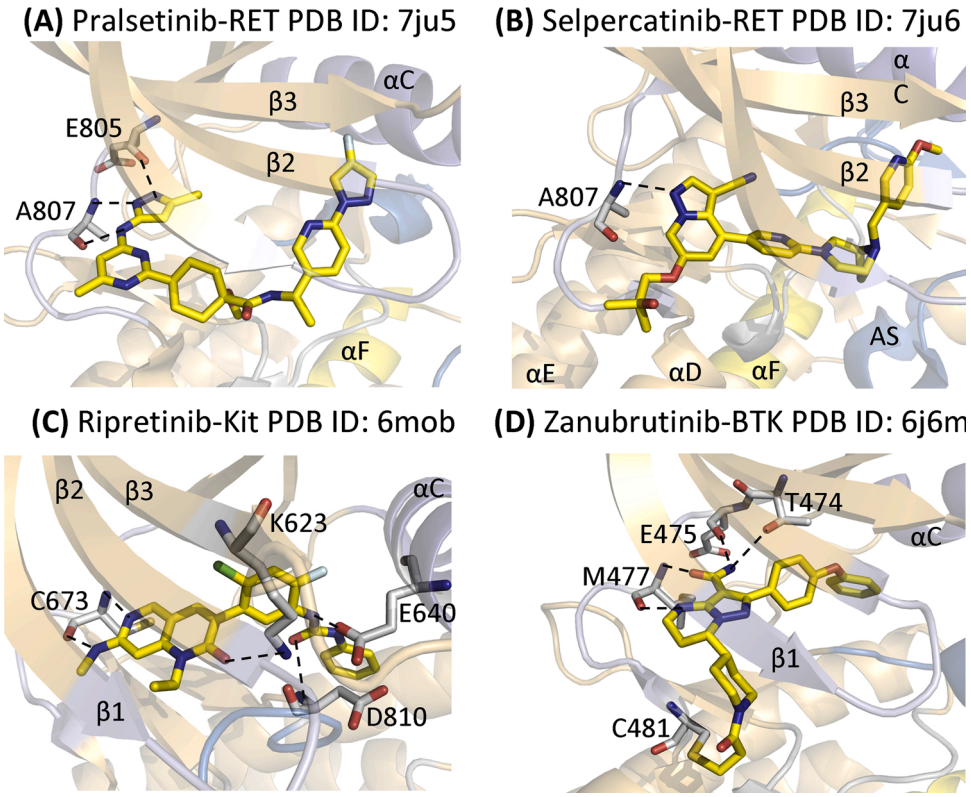

Fig. 7. (A) Pralsetinib-RET. (B) Selpercatinib-RET. (C) Ripretinib-Kit. (D) Zanubrutinib-BTK. The drug carbon atoms are colored yellow and the dashed lines represent polar bonds. AS, activation segment.

hydrophobically with G731, E732, G733, G736 of the G-rich loop, K737 and V738 of the β2-strand, AxK-K758 and L760 of the β3-strand, D771 and L772 of the αC-helix, and ^{805}EYAKYG^{810} of the hinge-linker segment. The drug binds to the front pocket and the FP—II subpocket of an active enzyme form and is thus classified as a type I inhibitor [24]. The overall clinical effectiveness of selpercatinib and pralsetinib is very similar [60]. For a review of the function and structure of RET, see Ref. [34].

Ripretinib is a 1,6-naphthyridine-urea derivative (Fig. 6C) that is FDA-approved for the fourth-line treatment of patients with GIST (gastrointestinal stromal tumors). This malady is the most common sarcoma or mesenchymal tumor of the gastrointestinal tract [64]. Approximately 80–85 % of these tumors are the result of activating mutations in the *KIT* stem cell factor receptor proto-oncogene [65]. Additionally, point mutations in the *PDGFRA* gene result in the generation of an activated and oncogenic PDGFRα that occurs in around 5–7% of these neoplasms [66,67]. The *PDGFRA* and *KIT* mutations are mutually exclusive. Of clinical importance, targeted therapy with protein-tyrosine kinase antagonists has transformed the treatment of advanced or unresectable GIST over the last 15 years.

Heinrich et al. and Corless et al. discovered that the activating *PDGFRA* mutations are found within (i) the juxtamembrane segment (exon 12 V561D) preceding the protein kinase domain, (ii) the αC-β4 back loop of the amino-terminal lobe (exon 14 N659K), or (iii) the activation segment (exon 18 D842V/Y and Del 845–848) [64,66]. In contrast to the wild type receptor found in the plasma membrane, mutant PDGFRα is mis-localized within the endoplasmic reticulum where it can activate JAK-STAT signaling whereas the wild type receptor only weakly activates STAT signaling [68]. Resistance mutations are quite heterogeneous, with multiple secondary mutations arising in individual patients [67]. In those patients with metastatic or unresectable GIST, treatment with imatinib is efficacious in patients with *PDGFRα*

exon 12 and exon 14 mutations, but not those with the most prevalent exon 18 mutations [69]. Although PDGFRα D842V mutant proteins are insensitive to sunitinib inhibition [70], patients that do not respond to imatinib generally respond initially to sunitinib or regorafenib as effective second-line and third-line treatments regardless of *KIT* or *PDGFRA* mutational status [71].

Because of the universal development of resistance to imatinib, sunitinib, and regorafenib in patients with Kit- or PDGFRα-mediated GIST, other small molecule inhibitors have been developed including ripretinib for the treatment of drug resistant neoplasms. The IC_{50} value of ripretinib for both wild type Kit and wild type PDGFRα is about 3 nM [72]. In addition to the GIST targets of Kit and PDGFRα, ripretinib is a multikinase inhibitor with activity against PDGFRβ, Tie2, VEGFR2 and B-Raf. For more information on the nature of Kit and the PDGFRs, see Refs. [32,33]. For data derived from the clinical trials that led to the FDA-approval of ripretinib for the fourth-line treatment of GIST that is independent of the mutational status of *KIT* or *PDFGRα*, see Ref. [73].

Although we lack the X-ray crystal structure of ripretinib bound to Kit, we have the structure of a chlorine analogue, DP2976 (bearing a chlorine for bromine substitution on the phenyl ring), bound to the enzyme (PDB ID: 6mob) [72]. The structure shows that the methyl-amino nitrogen forms a hydrogen bond with the carbonyl group and the *N*6 of the naphthyridine forms a hydrogen bond with the N—H group of C673, the third hinge residue (Fig. 7C). The keto oxygen of the drug forms a hydrogen bond with the ε-amino group of the β3-strand K623. Moreover, the urea oxygen atom forms a hydrogen bond with the N—H group of DFG-D810 and one urea N—H group hydrogen bonds with the carboxyl group of αC-E640. The ligand makes hydrophobic contact with six spine residues (RS1/2/3, CS6/7/8), three shell residues (Sh1/2/3), and the KLIFS-3 residue (Table 6). The ligand also interacts hydrophobically with G596 of the G-rich loop, V622 and V623 of the β3-strand, E640, V643 of the αC-helix, and two residues (L647, I653) of the αC-β4 back loop. The compound also makes additional hydrophobic contact with E671, Y672, C673, and G676 of the hinge-linker segment, L783 of the αE-helix, I808 of the large lobe β8-strand, C809 (the x residue of xDFG), DFG-D810 and A814 of the activation segment. The ligand occupies the front pocket, gate area, back pocket, and BP-IA/B, BP-II-out, and BP-III. The drug binds to Kit with DFG-D_{out} and it extends into the back pocket and is thus classified as a type IIA inhibitor [24]. Because the only differences in the structures of DP2976 and ripretinib involve the substitution of chlorine for bromine, it is likely that the interaction of ripretinib with Kit is identical.

Zanubrutinib is an irreversible 4,5,6,7-tetrahydropyrazolo[1,5-*a*] pyrimidine derivative (Fig. 6D) that inhibits Bruton protein-tyrosine kinase and is FDA-approved for the treatment of mantle cell lymphomas [74,75]. These lymphomas are B cell disorders that make up about 6% of non-Hodgkin lymphomas and this disease usually presents with palpable lymphadenopathy at a median age of about 65 years [76]. About 70 % of patients are at stage IV at the time of diagnosis with bone marrow, spleen, peripheral blood, and gastrointestinal involvement. The male/female ratio is 4/1. The historical median overall survival in people with newly diagnosed mantle cell lymphomas is three to four years. The use of BTK inhibitors (zanubrutinib, ibrutinib, and acalabrutinib) in the treatment of B-cell-related hematological malignancies is regarded as a significant therapeutic breakthrough [11,37,60].

The X-ray crystal structure shows that the zanubrutinib pyrimidine NH— group forms a hydrogen bond with the carbonyl group of M477 and the carboxamide carbonyl group forms a hydrogen bond with the NH— group with this same third hinge residue [77]. The carboxamide NH— group forms hydrogen bonds with the —OH group of the gatekeeper T474 and the carbonyl group of E475 (Fig. 7D). Zanubrutinib makes hydrophobic contact with five spine residues (RS2/3 and CS6/7/8), three shell residues (Sh1/2/3), and the KLIFS-3 residue that occurs immediately before the G-rich loop. The inhibitor also makes hydrophobic contact with the β3-strand AIK-K430, hinge-linker residues Y476, M477, G480, C481, and the αD-helix residues L483 and N484. Zanubrutinib also makes hydrophobic contact with catalytic loop residue R525, S538 (the x of xDFG), DFG-D539, and L542 of the activation segment. Zanubrutinib occupies the front and back pockets and the intervening gate area and BP-I-B. The drug binds to an inactive enzyme with αC_{out}, DFG-D_{in}, and a closed activation segment. The antagonist forms a covalent linkage with C481 at the end of the hinge-linker segment and is accordingly classified as a type VI inhibitor [24].

Selumetinib is a methyl-benzimidazole-carboxamide derivative (Fig. 6E) that inhibits the dual specificity MEK1/2 protein kinases and is FDA-approved for the treatment of neurofibromatosis type-1 (NF1) patients with inoperable plexiform neurofibromas. The NF1 gene encodes neurofibromin, which is a large molecular weight protein (319 kDa) that stimulates the GTPase activity of Ras [78]. The mutated gene product is inactive, which allows cells to grow uncontrolled. The Ras-Raf-MEK-ERK MAP kinase signaling module participates in the control of numerous processes including cell proliferation, the regulation of apoptosis, and RNA synthesis and processing [41]. MEK1/2 activate ERK1/2 by first catalyzing the phosphorylation of Y204/187 and then T202/185. Both of these residues occur within the ERK1/2 activation segment and the phosphorylation of both is required for enzyme activation [42,43]. The only known Raf substrates are MEK1/2 and the only known MEK1/2 substrates are ERK1/2. In contrast, there are hundreds of ERK1/2 substrates [42,43]. The MAP kinase cascade is perhaps the most important oncogenic driver of human cancers and the blockade of this signaling module by targeted inhibitors such as selumetinib is an important antitumor strategy.

Neurofibromatosis-1 (von Recklinghausen disease) is a common autosomal dominant neurocutaneous genetic disease (1/3000 live births) that usually appears in childhood and the signs and symptoms are often noticeable at birth or shortly afterward [79]. This disorder is characterized by tumors in the nervous system and skin. Neurofibromas are benign tumors with mixed cell types including Schwann cells, perineural cells, and fibroblasts. Most affected children exhibit harmless light-brown flat café au lait spots that are present at birth or appear during the first years of life. Exhibiting more than six café au lait spots strongly suggests a diagnosis of NF1. Additional signs and symptoms of neurofibromatosis type 1 vary, but they can include high blood pressure (hypertension), short stature, an unusually large head (macrocephaly), and skeletal abnormalities such as an abnormal curvature of the spine (scoliosis).

Cafe-au-lait spots and neurofibromas are benign and do not require treatment. Surgical excision can be performed on symptomatic lesions, but recurrence can occur. Plexiform neurofibromas, which occur in 20–50 % of patients with this disorder, are usually present from birth [79]. They are similar to neurofibromas, but they arise from muscle nerve fascicles and can infiltrate into the surrounding structures. These neurofibromas can cause functional impairment and pain. Complete surgical resection is often impossible and the regrowth of the tumor after incomplete surgical resection is common. Plexiform neurofibromas have potent neoplastic potential with an 8–13 % risk to develop into malignant peripheral nerve sheath tumors. Malignant transformation should be suspected if there is a rapid increase in tumor size, change of the tumor from soft-to-hard, pain for longer than one month, or new neurologic deficits. These neoplasms are treated with wide local excision. Imatinib has been shown to decrease plexiform neurofibroma size, but selumetinib treatment is now the preferred option [80].

Neurofibromatosis type 2 (NF2) is a disease characterized by bilateral vestibular schwannomas (acoustic neuromas) and meningiomas [79]. The *NF2* gene encodes a 69.7 kDa protein that plays a pivotal role in tumor suppression by restricting proliferation and promoting apoptosis as a regulator of the Hippo/SWH (Sav/Wts/Hpo) signaling pathway. The incidence of NF2 is about 5% of that of NF1 (1/60,000 live births). Owing to the eighth cranial nerve involvement, these patients require assessment of their hearing. Surgery represents the first line treatment for symptomatic tumors, but the recurrence rate is 44 %. Bevacizumab, a monoclonal antibody directed against VEGF, is used to

Table 6
Drug-enzyme hydrophobic (Φ) and hydrogen-bond (A, D) interactions based upon their common KLIFS residue numbers[a,b,c,d,e].

	PDB ID	RS1	RS2	RS3	RS4	Sh1	Sh2	Sh3	CS5	CS6	CS7	CS8	KLIFS-3[d]	KLIFS pockets[a]
KLIFS no. → Drug-enzyme ↓		68	82	28	38	36	45	43	76	77	11	15	3	
Type I inhibitors														
Bosutinib-Src	4mxo			Φ		Φ	Φ	Φ		Φ	Φ	Φ	Φ	F,G, BP-I-A/B
Brigatinib-ALK	6mx8			Φ			Φ			Φ	Φ	Φ	Φ	F, FP-I
Crizotinib-ROS	3zbf					Φ	Φ			Φ	Φ	Φ	Φ	F, FP-I
Dasatinib-Abl	2gqg			Φ		Φ	Φ, A	Φ		Φ	Φ	Φ	Φ	F, G, B, BP-I-A/B
Erlotinib-EGFR	1m17						Φ	Φ		Φ	Φ	Φ	Φ	F, G, B, BP-I-A/B
Gefitinib-EGFR	2ity			Φ			Φ	Φ		Φ	Φ	Φ	Φ	F,G, BP-I-A/B
Palbociclib-CDK6	2euf					Φ	Φ			Φ	Φ	Φ	Φ	F
Pralsetinib-RET	7ju5						Φ			Φ	Φ	Φ	Φ	F, FP-II
R406 (fostamatinib)-Syk	3fqs					Φ	Φ			Φ	Φ	Φ	Φ	F
Selpercatinib-RET	7ju6						Φ			Φ	Φ	Φ	Φ	F, FP-II
Tofacitinib-JAK1	3eyg					Φ	Φ			Φ	Φ	Φ	Φ	F, FP-I/II
Tofacitinib-JAK3	3lxk					Φ	Φ		Φ	Φ	Φ	Φ	Φ	F, FP-I/II
Vandetanib-RET	2ivu				Φ	Φ	Φ	Φ		Φ	Φ	Φ	Φ	F,G, BP-I-A/B
Type I½A inhibitors														
Dabrafenib–B-Raf	5csw		Φ, D	Φ	Φ	Φ	Φ	Φ		Φ	Φ	Φ	Φ	F, G, B, BP-I-A/B, BP-II-in, BP-II-A-in
Erdafitinib	5ew8		Φ	Φ		Φ	Φ	Φ		Φ	Φ	Φ	Φ	F, G, B, BP-I-A/B
Lapatinib-EGFR	1xkk		Φ	Φ	Φ	Φ	Φ	Φ		Φ	Φ	Φ	Φ	F, G, B, BP-I-A/B, BP-II-in, BP-II-A-in
Lenvatinib-VEGFR	3wzd		Φ	Φ		Φ	Φ			Φ	Φ	Φ	Φ	F, G, B, BP-I-B, BP-II-in
Palbociclib-CDK6	5l2i					Φ	Φ			Φ	Φ	Φ	Φ	F
Vemurafenib-B-Raf	3og7		Φ	Φ	Φ	Φ	Φ	Φ		Φ	Φ	Φ	Φ	F, G, B, FP-I, BP-I-A/B, BP-II-in, BP-II-A-in
Type I½B inhibitors														
Abemeciclib-CDK6	5l2s					Φ	Φ			Φ	Φ	Φ	Φ	F, FP-II
Alectinib-ALK	3aox					Φ	Φ			Φ	Φ	Φ	Φ	F, BP-I-B
Ceritinib-ALK	4mkc			Φ		Φ				Φ	Φ	Φ	Φ	F, FP-I
Crizotinib-ALK	2xp2			Φ			Φ			Φ	Φ	Φ	Φ	F, FP-I
Crizotinib-Met	2wgj			Φ		Φ	Φ			Φ	Φ	Φ	Φ	F, FP-I
Entrectinib-TRKA	5kvt					Φ	Φ		Φ	Φ	Φ	Φ	Φ	F, FP-I
Erlotinib-EGFR	4hjo			Φ		Φ	Φ			Φ	Φ	Φ	Φ	F, G, BP-I-A/B
Lorlatinib-ALK	4cli									Φ	Φ	Φ	Φ	F, FP-I
Ribociclib-CDK6	5l2t					Φ	Φ			Φ	Φ	Φ	Φ	F, G, FP-I
Type IIA inhibitors														
Axitinib-VEGFR	4ag8		Φ	Φ		Φ	Φ	Φ		Φ	Φ	Φ	Φ	F, G, B, BP-I-B, BP-II-out
Imatinib-Abl[f]	1iep	Φ, A	Φ	Φ		Φ	Φ, A	Φ		Φ	Φ	Φ	Φ	F, G, B, BP-I-A/B, BP-II-out, BP-IV
Imatinib-Kit	1t46	Φ	Φ	Φ		Φ	Φ, A	Φ		Φ	Φ	Φ	Φ	F, G, B, BP-I-A/B, BP-II-out, BP-IV
Nilotinib-Abl	3cs9	Φ	Φ	Φ		Φ	Φ, A	Φ		Φ	Φ	Φ	Φ	F, G, B, BP-I-A/B, BP-II-out, BP-V
Pexidartinib-CSF1R	4r7h		Φ	Φ		Φ	Φ			Φ	Φ	Φ	Φ	F, G, B, BP-I-B, BP-II-out, BP-V
Ponatinib-Abl[f]	3oxz	Φ, A	Φ	Φ		Φ	Φ	Φ		Φ	Φ	Φ	Φ	F, G, B, BP-I-A/B, BP-II-out, BP-III, BP-IV
Ponatinib-Kit	4u0i	Φ, A	Φ	Φ		Φ	Φ	Φ		Φ	Φ	Φ	Φ	F, G, B, BP-II-A/B, BP-II-out, BP-III, BP-IV
Ponatinib-B-Raf	1uwh	Φ	Φ	Φ		Φ	Φ			Φ	Φ	Φ	Φ	F, G, B, BP-I-B, BP-II-out, BP-III
Ripretinib-Kit	6mob	Φ	Φ	Φ		Φ	Φ	Φ		Φ	Φ	Φ	Φ	F, G, B, BP-I-A/B, BP-II-out, BP-III
Sorafenib-CDK8	3rgf	Φ	Φ	Φ		Φ	Φ			Φ	Φ	Φ	Φ	F, G, B, BP-I-B, BP-II-out, BP-III
Sorafenib-VEGFR	4asd	Φ	Φ	Φ		Φ	Φ			Φ	Φ	Φ	Φ	F, G, B, BP-I-B, BP-II-out, BP-III
Type IIB inhibitors														
Bosutinib-Abl	3ue4		Φ	Φ		Φ	Φ	Φ		Φ	Φ	Φ	Φ	F, G, BP-II-A/B
Gilteritinib-FLT3	6jqr		Φ							Φ	Φ	Φ	Φ	F
Nintedanib-VEGFR2	3c7q			Φ		Φ	Φ			Φ	Φ	Φ	Φ	F, G, BP-I-B
Sunitinib-Kit	3g0e		Φ			Φ				Φ	Φ	Φ	Φ	F
Sunitinib-VEGFR	4agd		Φ			Φ	Φ			Φ	Φ	Φ	Φ	F, BP-I-B
Type III inhibitors														
Cobimetinib-MEK1	4an2		Φ			Φ	Φ	Φ						G, B, BP-II-in
Selumetinib-MEK1	4u7z		Φ			Φ	Φ	Φ						G, B, BP-II-in
Type VI inhibitors														
Afatinib-EGFR	4g5j			Φ			Φ	Φ		Φ	Φ	Φ	Φ	F, G, BP-I-A/B
Dacomitinib-EGFR	4i24						Φ	Φ		Φ	Φ	Φ	Φ	F, G, BP-I-B
Ibrutinib-BTK	5p9j		Φ	Φ		Φ	Φ	Φ		Φ	Φ	Φ	Φ	F, G, B, BP-I-B
Neratinib-EGFR	2jiv		Φ	Φ	Φ	Φ	Φ	Φ		Φ	Φ	Φ	Φ	F, G, B, BP-I-A/B
Osimertinib-EGFR	6jxt									Φ	Φ	Φ	Φ	F
Zanubrutinib-BTK	6j6m		Φ	Φ		Φ	Φ	Φ		Φ	Φ	Φ	Φ	F, G, B, BP-I-B

[a] Klifs.net.
[b] Human enzyme unless otherwise noted.
[c] Drugs not previously reviewed (Refs [9,10]) are indicated in **bold** print.

[d] KLIFS-3, kinase-ligand interaction fingerprint and structure residue-3.
[e] A, hydrogen-bond acceptor; D, hydrogen-bond donor.
[f] Mouse enzyme.

treat neurofibromatosis type 2 patients medically. It decreases tumor size and improves hearing in about one-half of the cases.

Selumetinib is a selective inhibitor of MEK1/2 with an IC_{50} value of about 8 nM (klifs.net). Like cobimetinib, selumetinib is not an ATP steady-state inhibitor and it binds to MEK1/2 at an allosteric site near the ATP-binding pocket. Owing to the importance of the Ras-Raf-MEK-ERK MAP kinase pathway in many cancers, selumetinib is in more than 100 clinical trials (ClinicalTrials.gov). Disease targets include myelofibrosis, acute lymphoblastic and chronic myelogenous leukemias, non-Hodgkin lymphomas, astrocytomas, gliomas, melanomas, soft tissue sarcomas, pancreatic, biliary tract, colorectal, breast, endometrial, differentiated thyroid, hepatocellular, and non-small cell carcinomas. Cobimetinib, binimetinib, and trametinib are MEK1/2 inhibitors that are FDA-approved for the treatment of melanomas and trametinib is also approved for the treatment of NSCLC with *BRAF* mutations.

Robarge et al. solved the X-ray crystal structure of selumetinib and AMPPNP (adenylyl imidodiphosphate) bound to MEK1 [81]; that both an ATP analog and the drug can bind simultaneously to the same enzyme conformation indicates that selumetinib is an allosteric inhibitor. Selumetinib forms three hydrogen bonds with the ε-amino group of ARK-K97 and one hydrogen bond with the amide group of S212, the 5th activation segment residue (Fig. 8). The compound makes hydrophobic contact with one spine residue (RS2) and all three shell residues. It also makes hydrophobic contact with N78 of the glycine-rich loop, β3 ARK-K97, L115 and L118 of the αC-helix, C207 (the x of xDFG), and D208, G210, S212, L215, and I216 of the activation segment. AMPPNP, the ATP analog, forms hydrogen bonds with the first and third hinge residues (E144, M146) and the ribose moiety forms a hydrogen bond with S150 at the end of the hinge-linker segment. The analog makes hydrophobic contact with four spine residues (RS2, CS6/7/8), one shell residue (Sh2), and the KLIFS-3 residue. It also makes hydrophobic contact with G75 and A76, within the glycine-rich loop, E144 and S150 within the hinge-linker segment, and Q153 within the αD-helix. Additionally, it makes hydrophobic contact with K192 and S194 within the catalytic loop. The drug is found within the front pocket, gate area, back pocket, BP-I-B and BP-II-in. Selumetinib is bound to an inactive enzyme form with a closed activation segment and with αC_{out}. The drug occurs next to the ATP-binding pocket and is classified as a type III allosteric inhibitor [24]. Type IV allosteric inhibitors bind far from the ATP-binding site.

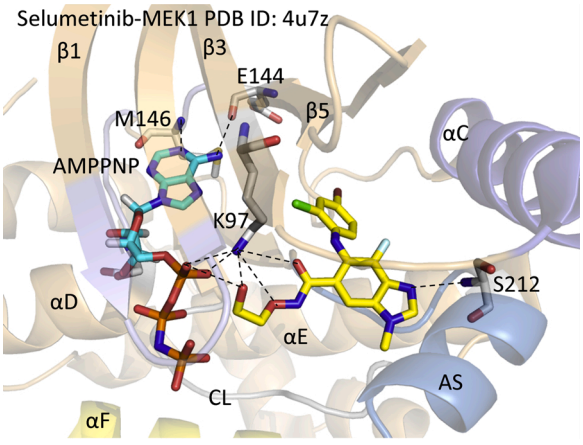

Fig. 8. Selumetinib-MEK1. AS, activation segment. AMPPNP (adenylyl imidodiphosphate) is an ATP-analog. The drug carbon atoms are colored yellow and the dashed lines represent polar bonds. AS, activation segment.

5. Newly approved protein kinase antagonists without drug-enzyme structures

Avapritinib is a pyrrolo-pyrimidine derivative (Fig. 6F) that is FDA-approved for the fourth-line treatment of GISTs bearing *PDGFRα* activation segment exon 18 mutations. Exon 18 encodes activation segment residues 3–15 beginning with the DFG-G residue and such mutations are thought to lead to the activation of PDGFRα. The most common activation segment mutation is the D842V substitution involving the 7th residue following DFG-D. These activation segment mutations are resistant to imatinib, sunitinib, regorafenib and ripretinib, which represent the initial small molecule targeted treatments. These four drugs likely bind to and inhibit the inactive DFG-D_{out} conformation of their target enzymes. Treatment guidelines recommend mutational testing before beginning therapy because the presence or absence and types of *KIT* and *PDGFRA* mutations affect the clinical response to multitargeted protein-tyrosine kinase inhibitors. For example, patients with GIST bearing *KIT* exon 9 mutations may benefit from high-dose imatinib therapy or from sunitinib therapy[82]. Despite these findings, Florindez and Trent reported that only about one-quarter of the patients with GIST in the United States undergo such mutational testing [83]. Patients bearing the *PDGFRA* exon 18 D842V mutation have a poor prognosis, but this situation has improved following the introduction of avapritinib [82]. Gardino et al. reported that the avapritinib IC_{50} for $PDGFR\alpha^{D842V}$, which occurs in about 75 % of all *PDGFRα* mutant tumors, was 0.24 nM [84]. Owing to its effectiveness, avapritinib is FDA-approved for the treatment of *PDGFRα* exon 18-mutant GIST [60, 82].

Capmatinib is an imidazo[1,2-*b*]triazine derivative (Fig. 6G) that is FDA-approved for the treatment of NSCLC bearing *MET* exon 14 skipping mutations [60,85]. MET is a receptor protein-tyrosine kinase whose activating ligand is hepatocyte growth factor (HGF) [25]. MET was initially discovered as an oncogenic TPR-MET fusion protein where TPR refers to translocated promoter region [86]. MET originally represented the methyl group in the carcinogen (*N*-methyl-N′-nitroso-guanidine) used to generate the fusion protein in a human osteogenic sarcoma cell line [86]. Physiologically, MET promotes morphogenesis, wound repair, tissue remodeling, and organ homeostasis [87]. MET plays a role in promoting cell division, survival, and metastasis of cancer cells. MET has been used as an acronym for “mesenchymal-epithelial transition” factor [88] or an abbreviation for "metastasis.” Although MET and HGF are found in many different tissues, MET is characteristically expressed in epithelial cells while HGF is expressed in mesenchymal cells [89].

MET is a typical receptor protein-tyrosine kinase that consists of an extracellular ligand-binding domain, a transmembrane segment, a juxtamembrane segment, a protein kinase domain, and a carboxyterminal tail [87]. Following HGF binding and receptor dimerization, protein kinase activity is activated following the phosphorylation of Tyr1234 and Tyr1235 in the enzyme activation segment. Following activation, MET mediated phosphorylation of two tyrosine residues (Tyr1349 and Tyr1356) in the carboxyterminal tail provides binding sites for signal-transduction docking proteins including Gab1, Grb2, PLC, and Src. Liu et al. demonstrated that MET activity increases the expression of EGFR, ErbB3, and their ligands in cells in culture [89]. Moreover, these investigators also found that capmatinib blocks these stimulatory actions. Table 1 contains a list of the selected residues in the MET protein kinase domain that are catalytically important and Table 2 contains a list of the residues that make up the spine and shell residues.

A large number of disorders including lymphomas and rhabdomyosarcomas exhibit sustained MET activation owing to stimulation, overexpression, or mutations [90,91]. Moreover, activating MET protein kinase domain point mutations occur in sporadic and inherited human

hepatocellular, renal, and head and neck carcinomas [92–94]. Furthermore, *MET* exon 14 skipping mutations occur in 3–4 % of patients with NSCLC that result in the production of a smaller protein that is deficient in residues in the juxtamembrane segment; residues encoded by exon 14 include ^{1000}SVDYRATFPE^{1009}. These mutant proteins are processed more slowly by the ubiquitin-proteosome pathway leading to increased stability and activity. Capmatinib is a potent inhibitor of the exon 14 mutants as well as the wild type enzyme with a K_i value of 0.31 nM. See Refs. [25,27] for a summary of the properties of MET and Refs. [60,85] for a summary of the clinical trials that lead to the FDA-approval of capmatinib for the treatment of NSCLC with MET exon 14 skipping mutations. Owing to the general role of MET in the pathogenesis of various cancers, capmatinib is in clinical trials for the treatment of additional cancer types including those of glioblastomas, colorectal cancers, renal cell carcinomas, hepatocellular carcinomas, squamous cell carcinomas of the head and neck, triple negative breast cancers, and melanomas (ClinicalTrials.gov).

Pemigatinib is a tetrazatricyclotrideca-1,3,6,8-tetraene derivative (Fig. 6H) that is approved for the first-line treatment of patients with advanced or unresectable cholangiocarcinomas bearing an FGFR2 fusion protein or other genetic rearrangement [60,95,96]. The human fibroblast growth factor family consists of 22 factors and five transmembrane receptors [31]. Of the 22 factors, eighteen are secreted while four of them function exclusively within the cell. Four of the fibroblast growth factor receptors (FGFRs) possess intracellular protein-tyrosine kinase activity while the fifth (FGFRL1) has a short 105-residue intracellular non-enzymatic component. *FGFR* gene alterations occur in a wide variety of cancers including those of the urinary bladder, breast, ovary, prostate, endometrium, lung, and stomach. The majority (66 %) of *FGFR* gene alterations involve gene amplifications, followed by mutations (26 %), and rearrangements that produce fusion proteins (8%).

Cholangiocarcinomas are malignancies of the biliary duct system that may occur in the liver or extrahepatic bile ducts [97]. The bile duct and pancreatic ducts empty into the duodenum at the ampulla of Vater. These carcinomas occur in three anatomic regions: intrahepatic, extrahepatic (i.e., perihilar), and distal extrahepatic occurring near the small intestine. Perihilar tumors are the most common and intrahepatic tumors are the least common form of these malignancies. Distal extrahepatic tumors are located near the upper border of the pancreas and they may extend to the ampulla. More than 95 % of these tumors are classified histologically as ductal adenocarcinomas. Complete surgical resection is the only therapy affording a chance of cure for cholangiocarcinomas; unfortunately, most patients present with unresectable or metastatic disease. Symptoms of cholangiocarcinoma may include abdominal pain, yellow skin (jaundice), weight loss, generalized itching, and fever owing to bile duct obstruction and inflammation. Several cholangiocarcinoma FGFR2-fusion proteins have been described including FGFR2-NOL4, FGFR2-KIAA1598, FGFR2-BICC1, and FGFR2-TACC3 [31]. A *FGFR2* C382R mutation within the receptor transmembrane segment has also been reported.

A variety of other neoplasms resulting from *FGFR1/2/3/4* gene alterations have been reported. About 54 % of head and neck squamous cell carcinomas, 46 % or urothelial cancers, 47 % of gastric cancers, 46 % of squamous cell lung carcinomas, 42 % of uterine cervical cancers, 39 % of lung adenocarcinomas, 38 % of melanomas, 35 % of breast adenocarcinomas, 22 % of prostate adenocarcinomas, and 17 % of colorectal adenocarcinomas possess such mutations [31]. In addition to pemigatinib, erdafitinib is an FDA-approved FGFR antagonist that is used for the treatment of urothelial cancers and nintedanib is used for the treatment of idiopathic pulmonary fibrosis, diseases associated with increased FGFR activity. Moreover, pazopanib is a multikinase inhibitor with activity against FGFR1/3 that is approved for the treatment of renal cell carcinomas and regorafenib is a multikinase inhibitor with activity against FGFR1/2 that is approved for the treatment of colorectal cancer and GIST. Owing to the large variety and significant frequency of neoplasms whose pathogenesis is related to FGFFR dysregulation, this enzyme family represents an import therapeutic target. The drug is currently in 20 clinical trials targeting acute myelogenous leukemias, NSCLC, endometrial, breast, and gastrointestinal cancers (ClinicalTrials.gov).

Tucatinib is a quinazoline-triazolo[1,5-*a*]pyridine derivative (Fig. 6I) that is FDA-approved as a combination second-line treatment with trastuzumab and capecitabine for patients with unresectable or metastatic HER2-positive breast cancer, including those patients with brain metastases [60,98]. Breast carcinomas are the leading cause of death from malignancies that occur predominantly (breast) or exclusively (ovary, uterine corpus, uterine cervix) in women in the United States and worldwide [99,100]. About 20 % of advanced breast cancer cases are HER2-positive [101]. ErbB2 overexpression was correlated with a poor prognosis prior to the advent of ErbB2 targeted therapies. The standard first-line treatment for this disorder includes pertuzumab and trastuzumab in combination with a taxane such as docetaxel or paclitaxel [102]. Pertuzumab is a monoclonal antibody that binds to ErbB2/HER2 and prevents its dimerization with other ErbB family members. Trastuzumab is a monoclonal antibody that binds to the extracellular domain of ErbB2/HER2 and results in HER2 internalization and down-regulation, a process that stimulates immune cells to kill the HER2-expressing cell. The taxanes are antimitotic drugs that enhance microtubule polymerization and inhibit their function. Capecitabine is a prodrug that is metabolized to 5-flurorouracil, which inhibits thymidylate synthase, DNA synthesis and function, and RNA function.

Tucatinib is a selective inhibitor of ErbB2 with an IC_{50} value of 6.9 nM compared with an EGFR value of 449 nM; this selectivity is even greater when tested in cells in culture [103]. A biochemical screen against 223 protein kinases confirmed the selectivity of tucatinib. Lapatinib and neratinib, which are FDA-approved for the treatment of HER2-positive breast cancer, are equipotent against EGFR and ErbB2. The off-target inhibition of EGFR may contribute to the toxicity of these two drugs. Kulukian et al. found that the combination of tucatinib with trastuzumab was more effective in inhibiting the growth of cell lines overexpressing HER2 [103]. Moreover, Murthy et al. reported that the addition of tucatinib with trastuzumab and capecitabine was more effective in the treatment of HER2-positive metastatic breast cancer than the combination therapy without tucatinib [104]. HER2 overexpression has been reported in 6–37 % of gastric cancers and 5% of colon cancers. Clinical trials using tucatinib for the treatment of these disorders along with neoplasms of the uterine cervix, biliary tract, colorectal, and esophageal cancers and angiosarcomas are underway (ClinicalTrials.gov).

Upadacitinib is a tetrazatricyclo-dodeca-pentaene derivative (Fig. 6J) that is approved by the FDA for the second-line treatment (after methotrexate) of adults with moderately to severely active rheumatoid arthritis [105,106]. Rheumatoid arthritis (RA) is a relatively common disease of unknown etiology that affects about 1% of the adult population [107] with a female: male ratio of about 3:1 [108,109]. Patients with active rheumatoid arthritis incur joint damage, disability, decreased quality of life, and they may exhibit cardiovascular and other co-morbidities [107]. The pathogenic mechanisms for the development of rheumatoid arthritis result from a complex interplay of immunological, environmental, and genetic factors that produce dysregulation of the immune system and a breakdown of self-tolerance [110].

Disease-modifying antirheumatic drugs (DMARDs), which are key therapeutic agents, along with low doses of glucocorticoids such as prednisone reduce synovial and systemic inflammation. The leading DMARD is methotrexate, which can be combined with other drugs such as sulfasalazine and leflunomide [111]. Methotrexate (amethopterin) is a folate antagonist that inhibits purine, pyrimidine, and thymidine biosynthesis; the drug also inhibits enzymes involved in purine catabolism resulting in the accumulation of adenosine thereby leading to inhibition of T cell and B cell activity. The mechanism responsible for the anti-inflammatory activity of sulfasalazine is unclear. Leflunomide

inhibits dihydroorotate dehydrogenase and thereby inhibits pyrimidine synthesis.

Biological agents are used for the treatment of uncontrolled rheumatoid arthritis or when toxic effects arise with DMARDs [107]. Infliximab, which inhibits the action of tumor necrosis factor-α, was the first biological agent approved for inflammatory disease and this was followed by a variety of other biologics including adalimumab, abatacept, etanercept, rituximab, and tocilizumab. Infliximab (a mouse-human chimeric construct) and adalimumab (a human construct) are two monoclonal antibodies directed against TNF-α (tumor necrosis factor-α). Abatacept is a fusion protein composed of the Fc region of the immunoglobulin IgG1 fused to the extracellular domain of CTLA-4 (a protein receptor that down-regulates the immune response) while etanercept is a protein that functions as a decoy receptor that binds TNF-α. Rituximab is a chimeric human-mouse monoclonal antibody against CD20 that destroys B cells, which express CD20. Tocilizumab is a chimeric human-mouse monoclonal antibody directed against the membrane and soluble forms of the IL-6 receptor. There are at least 20 additional biosimilars that are either approved or are in clinical trials for the treatment of inflammatory disorders [112].

The Janus kinase (JAK) family of protein-tyrosine kinases is made up of four members: JAK1/2/3 and TYK2 (Tyrosine kinase 2) [40]. These non-receptor protein-tyrosine kinases share seven distinct JAK homology (JH1-JH7) domains. These enzymes contain an inactive amino-terminal pseudokinase domain (JH2) next to a functional carboxyterminal protein kinase domain (JH1). The pseudokinase domain typically inhibits the functional protein kinase domain. Janus is a two-faced (looking forwards and backwards) Roman God whose name was applied to this enzyme family because of the existence of the two protein kinase domains within a single polypeptide chain. JAK was previously formulated in a whimsical fashion as Just Another Kinase [113]. JAK1/2 and TYK2 are ubiquitously expressed in nearly all cell types whereas JAK3 is confined to hematopoietic, myeloid, and lymphoid cells [114]. The Janus kinases play an important role in normal hematopoiesis; accordingly, Janus kinase dysregulation can result in a variety of hematological illnesses.

The JAK-STAT (signal transducer and activator of transcription) pathway transduces extracellular signals from a variety of cytokines, growth factors, and hormones to the nucleus and is responsible for the expression of hundreds of protein-encoding genes [115]. The conversion of an extracellular signal into a transcriptional response involves several steps. First, ligand binding to cytokine receptors results in JAK activation following phosphorylation of two tyrosine residues within the activation segment of the JH1 domain as catalyzed by a partner Janus kinase enzyme. Next, the JH1 domain catalyzes the phosphorylation of tyrosine residues within the cytokine receptor that attracts the SH2 domain of STATs. The JH1 domain subsequently catalyzes the phosphorylation of the STAT molecules themselves. Then phosphorylated STATS dimerize and are translocated into the nucleus where they facilitate the transcription of target genes.

The JAK family is involved in a diverse range of physiological functions including cytokine and growth factor signaling [40]. The members of this family possess overlapping and unique functions. IL-6 signaling is important in the pathogenesis of rheumatoid arthritis and results in the activation of JAK1/2 and TYK2 with JAK1 playing a predominant role. Erythropoietin receptor signaling favors JAK2 for signal transduction and this combined activity plays a critical role in the development and deployment of reticulocytes and erythrocytes. JAK 3 along with JAK1 represent an important component in signal transduction for the cytokine receptors that possess a common γ-chain including IL-2/4/7/9/15/21. These cytokines are involved in T cell and natural killer (NK) cell survival.

Parmentier et al. designed upadacitinib as a selective JAK1 antagonist by focusing on differences of the G-rich loop of JAK enzymes [116]. The IC_{50} values for JAK1 (45 nM), JAK2 (109 nM), JAK3 (2100 nM), and TYK2 (4700 nM) as determined using enzyme assays demonstrated two-fold selectivity of JAK1 vs. JAK2; the IC_{50} value for JAK1 of 45 nM is greater than the low nanomolar values usually exhibited by therapeutic protein kinase antagonists. Using cell-based assays, however, these investigators found that the IC_{50} for the four enzymes for JAK1/2/3 and TYK2 was 14 nM, 593 nM, 1860 nM, and 2720 nM, respectively, demonstrating selectivities of 1,48,133, and 194-fold, respectively. These investigators found that upadacitinib inhibited JAK1-dependent signaling dependent upon IL-2, IL-6, and interferon-γ more effectively than it inhibited JAK2-dependent erythropoietin signaling.

Tofacitinib was the first protein kinase antagonist approved for the treatment of rheumatoid arthritis that inhibits JAK1/2/3 with equal low nanomolar IC_{50} values and baricitinib was the second protein kinase inhibitor that was approved for the treatment of rheumatoid arthritis that inhibits JAK1/2 and TYK2 inhibitor with nanomolar IC_{50} values. McInnes et al. compared the efficacy of these two antagonists with that of upadacitinib in human leukocytes [117]. For IL-2/3/15/21 JAK1/3-dependent cytokines in mononuclear cells, upadacitinib and tofacitinib were the most potent and equivalent (IC_{50} values of about 10–20 nM) and baricitinib was the least potent (IC_{50} values of 30–65 nM). For the blockade of JAK2 and TYK2-dependent IL-3 and granulocyte/macrophage colony stimulating factor signal transduction, upadacitinib and baricitinib were the most potent (IC_{50} values of about 12–84 nM) and tofacitinib was the least potent (about 100 nM). For the inhibition of JAK1/2 and TYK2 dependent IL-6/10 and interferon-α/γ signaling in $CD4^+$ T-cells, baricitinib, upadacitinib, and tofacitinib exhibited similar IC_{50} values (ranging from 23 to 132 nM).

Although upadacitinib was developed as a selective JAK1 inhibitor, it was the most potent inhibitor of the JAK2-dependent IL-3 and granulocyte/macrophage colony stimulating factor signal transduction in monocytes [117]. This study also demonstrated that tofacitinib moderately inhibits JAK2 as well as JAK1/3. These results indicate that information on the selectivity of protein kinases based upon in vitro kinase assays may differ from the data of biologically relevant cellular systems. See Refs. [105,106] for a summary of the studies that lead to the approval of upadacitinib.

6. Analyses of the physicochemical properties of orally effective drugs

6.1. Lipinski's rule of five (Ro5)

Medicinal chemists and pharmacologists have searched for advantageous drug-like chemical properties that result in medicinals with oral therapeutic effectiveness. Lipinski's "rule of five" is an experimental and computational methodology that is used to estimate solubility, membrane permeability, and efficacy in the drug-development setting [118]. It is a rule of thumb that assesses drug-likeness and determines whether a compound with specific pharmacological activities has physical and chemical properties that indicate it would make an orally effective agent. The Lipinski criteria were based upon data indicating that most orally effective medicinals are comparatively small and moderately lipophilic molecules. The Ro5 criteria are used during drug development as pharmacologically active lead compounds are serially optimized to increase their activity while maintaining their drug-like physicochemical properties and selectivity.

The Ro5 implies that less than ideal oral effectiveness is more likely to be found when (i) the calculated Log P (cLogP) is greater than 5, when (ii) there are greater than 5 hydrogen-bond donors, when (iii) there are greater than 5 × 2 or 10 hydrogen-bond acceptors, and when (iv) the molecular weight is greater than 5 × 100 or 500 [55]. The partition coefficient (P) is the ratio of the solubility of the un-ionized drug in the organic phase of water-saturated n-octanol divided by its solubility in the aqueous phase. The P value reflects the hydrophobicity of a compound; the larger the P value, the greater the hydrophobicity. The number of hydrogen-bond donors is easy to calculate and is the sum of NH and OH groups. The number of hydrogen-bond acceptors is more

difficult to determine as it consists of any heteroatom lacking a formal positive charge with the exception of heteroaromatic oxygen and sulfur atoms, pyrrole nitrogen atoms, halogen atoms, and higher oxidation states of nitrogen, phosphorus, and sulfur, but it includes the oxygen atoms bonded to them. The Ro5 is based on the chemical and physical properties of more than two thousand reference medicinals [118].

Excluding the macrolides (everolimus, sirolimus, and temsirolimus), the average molecular weight (MW) of the orally effective FDA-approved protein kinase inhibitors is 479 ranging from 306 (ruxolitinib) to 615 (trametinib) (Table 7). The compounds with a molecular weight greater than 500 include the three macrolides and fostamatinib (a prodrug that is converted to R406 with a molecular weight of 470), entrectinib, encorafenib, fedratinib, ceritinib, midostaurin, abemaciclib, ripretinib, bosutinib, brigatinib, cabozantinib, cobimetinib, nilotinib, dabrafenib, gilteritinib, ponatinib, lapatinib, neratinib, nintedanib, selpercatinib, and trametinib. Although this data shows that there is a tendency for orally effective small molecule protein kinase medicinals to exceed the 500 Da molecular-weight criterion, the masses of the larger compounds are still close to 500 Da. Moreover, eight of the 62 approved drugs have a cLogP of greater than five; these include cobimetinib, neratinib, abemaciclib, brigatinib, midostaurin, vandetanib, entrectinib, and ceritinib, but none of the 10 recently approved drugs has a cLogP greater than five. Moreover, the three macrolides (sirolimus, everolimus, and temsirolimus), dabrafenib, and fostamatinib have more than ten hydrogen bond acceptors. Thus, a total of 25 of the 62 FDA-approved small molecule protein kinase inhibitors fail to conform to Lipinski's Ro5.

6.2. The importance of lipophilicity and ligand efficiency

6.2.1. Lipophilic efficiency, LipE

After the emergence of Lipinski's Ro5 in 2001 [118], subsequent work on the physicochemical properties of orally effective medicinals has led to several refinements [119–126]. For example, lipophilic efficiency, or LipE, is a property that is used in drug development and discovery that combines potency and lipophilic-driven binding as a tactic to increase binding efficacy. The following formulas are used for calculating lipophilic efficiency:

$$\text{LipE} = \text{p}IC_{50} - \text{cLogD} \text{ or } \text{LipE} = \text{p}K_i - \text{cLogD}$$

Similar to its usage as expressing the molar hydrogen ion concentration as pH, the operator p denotes the negative of the Log_{10} of the IC_{50} or K_i. Furthermore, cLogD is the calculated Log_{10} of the Distribution coefficient; this parameter denotes the ratio of the drug solubility (both ionized and un-ionized) in the organic phase divided by its solubility in the aqueous phase of immiscible n-octanol/water at a specified pH, which is generally near 7.

The second term of the equation (– cLogD or minus cLogD) characterizes the lipophilicity of a medicinal where c indicates that the value is calculated using an algorithm based upon the properties of thousands of reference organic compounds. The greater the solubility of a compound in the organic phase of an immiscible n-octanol/water mixture, the more negative is the – cLogD and the greater is its lipophilicity. Leeson and Springthorpe postulated that drug lipophilicity, as assessed by its – cLogP value, is one of the more important properties that should be monitored during the drug development and discovery process [121]. Their use of – cLogP was based upon experiments performed before the use of the distribution coefficient (D) became in common use. For practical considerations, either cLog_{10}D or cLog_{10}P can be employed to compare a series of several compounds.

A higher lipophilicity may play a significant role in facilitating binding to adventitious targets that may lead to an increased number of adverse events. One objective for developing advantageous properties during drug development is to increase potency without simultaneously increasing lipophilicity. Lipophilic efficiency aids in the optimization of lead compounds by facilitating a direct comparison of drug congeners; furthermore, the same assay should be used to make such comparisons valid [124]. To cite one successful example, progress in the optimization during the development of crizotinib from lead compounds as described by Cui et al. was monitored by using lipophilic efficiency as a numerical index of binding effectiveness [88]; crizotinib is used in the treatment of ALK-positive and ROS1-positive NSCLC.

cLogD can be calculated for related compounds by computer algorithms in a matter of minutes. Because experimental determinations of Log_{10}D are labor intensive, such measurements are performed in only select cases. Smith reported that optimal values of lipophilic efficiency values range from 5 to 10 [120]. Decreasing the lipophilicity and increasing potency during drug discovery and development generally produces medicines with better pharmacological properties. The average value of lipophilic efficiency for the 62 FDA-approved small molecule protein kinase inhibitors is 5.03 with a range from 2 (vandetanib) to 8.5 (tofacitinib) (Table 8). Half of the FDA-approved small molecule antagonists (31) have values that are less than 5 while the recommended optimal range is from 5 to 10.

6.2.2. Ligand efficiency, LE

The ligand efficiency (LE) is a property that relates potency, or binding affinity, to the number of non-hydrogen atoms (heavy atoms) of a medicinal. The following formula is used to calculate this parameter:

$$\text{LE} = \Delta G^{\circ\prime}/\text{N} = -\text{RT} \ln K_{eq}/\text{N} = -2.303\text{RT} \text{Log}_{10} K_{eq}/\text{N}$$

$\Delta G^{\circ\prime}$ is the standard free energy change of a drug binding to its enzyme target at neutral pH, R represents the universal gas constant or energy-temperature coefficient, (0.00198 kcal/degree-mol), T signifies the absolute temperature in degrees Kelvin, K_{eq} is the value of the equilibrium constant, and N represents the number of heavy atoms (non-hydrogen atoms) in the agent. Hopkins et al. reported that optimal values of ligand efficiency are greater than 0.3 kcal/mol [119,123]. The K_i or IC_{50} values are surrogates for the equilibrium constant. At a physiological temperature of 37 °C (310 K), this equation becomes – (2.303 × (0.00198 kcal/mol-K) ×310 K Log_{10} K_{eq})/N or – 1.41 Log_{10} K_{eq}/N. Ligand efficiency was initially suggested as a procedure for comparing ligand affinities based upon the average binding energy per atom. Furthermore, ligand efficiency is particularly useful in fragment-based drug discovery protocols and, like lipophilic efficiency, it aids in the selection of lead compound derivatives [124].

Ligand efficiency corresponds to the binding affinity per heavy atom of the ligand or drug of interest. The value of N is a surrogate for the molecular weight. The equation that defines ligand efficiency shows that the value is directly proportional to – Log_{10} K_{eq} (a positive number), or the binding affinity and inversely proportional to the number of heavy atoms. The values of ligand efficiency for the FDA-approved small molecule protein kinase inhibitors based upon representative IC_{50} values are provided in Table 8. With the exceptions of six drugs (entrectinib, fostamatinib, midostaurin, neratinib, nilotinib and nintedanib), the values have an optimal value greater than 0.3. The values for ligand efficiency (LE) and lipophilic efficiency (LipE) listed in Table 8 are based on data obtained under different experimental conditions. Consequently, these values cannot be used to make a direct comparison of the agents owing to the different assay conditions used to obtain the data. However, these results were derived from different drug discovery projects and are intended to provide representative values. The primary protein kinase families that are targeted by the FDA-approved drugs are also listed in Table 8.

6.2.3. Additional chemical descriptors of orally effective drugs

To improve criteria related to oral effectiveness, not-unexpectedly, the Ro5 has generated many extensions and corollaries. For example, Veber et al. reported that the polar surface area (PSA) and the number of rotatable bonds differentiates between agents that are orally active and

Table 7
Properties of FDA-approved small molecule inhibitors [a].

Drug	PubMED CID	Formula	MW (Da)	HD [b]	HA [c]	cLogP [a,d]	Rotatable bonds	PSA [e] (Å^2)	Ring count	Complexity [f]
Abemaciclib	46220502	$C_{27}H_{32}F_2N_8$	507	1	9	5.2	7	75	5	723
Acalabrutinib	71226662	$C_{26}H_{23}N_7O_2$	466	2	6	1.1	4	119	5	845
Afatinib	10184653	$C_{24}H_{25}ClFN_5O_3$	486	2	8	4.0	8	88.6	4	702
Alectinib	49806720	$C_{30}H_{34}N_4O_2$	483	1	5	4.7	3	72.4	6	867
Avapritinib	118023034	$C_{26}H_{27}FN_{10}$	499	1	9	2.9	5	106	6	752
Axitinib	6450551	$C_{22}H_{18}N_4OS$	386	2	4	3.8	5	96	4	557
Baricitinib	44205240	$C_{16}H_{17}N_7O_2S$	371	1	7	0.3	5	129	4	678
Binimetinib	10288191	$C_{17}H_{15}BrF_2N_4O_3$	441	3	7	2.6	6	88.4	3	521
Bosutinib	5328940	$C_{26}H_{29}Cl_2N_5O_3$	530	1	8	5.0	9	82.9	4	734
Brigatinib	68165256	$C_{29}H_{39}ClN_7O_2P$	584	2	9	5.2	8	85.9	5	835
Cabozantinib	25102847	$C_{28}H_{24}FN_3O_5$	501	2	7	4.5	8	98.8	4	795
Capmatinib	25145656	$C_{23}H_{17}FN_6O$	412	1	6	3.2	5	81.5	5	637
Ceritinib	57379345	$C_{28}H_{36}ClN_5O_3S$	558	3	8	6.0	9	114	4	835
Cobimetinib	16222096	$C_{21}H_{21}F_3IN_3O_2$	531	3	7	5.1	4	64.6	4	624
Crizotinib	11626560	$C_{21}H_{22}Cl_2FN_5O$	450	2	6	4.4	5	78	4	558
Dabrafenib	44462760	$C_{23}H_{20}F_3N_5O_2S_2$	520	2	11	4.5	6	148	4	817
Dacomitinib	11511120	$C_{24}H_{25}ClFN_5O_2$	470	2	7	4.8	7	79.4	4	665
Dasatinib	3062316	$C_{22}H_{26}ClN_7O_2S$	488	3	9	3.0	7	135	4	642
Encorafenib	50922675	$C_{22}H_{27}ClFN_7O_4S$	540	3	10	3.1	10	149	3	836
Entrectinib	25141092	$C_{31}H_{34}F_2N_6O_2$	561	3	8	5.5	7	85.5	6	847
Erdafitinib	67462786	$C_{25}H_{30}N_6O_2$	446	1	7	4.6	9	77.3	4	583
Erlotinib	176870	$C_{22}H_{23}N_3O_4$	393	1	7	3.1	11	74.7	3	525
Everolimus	6442177	$C_{53}H_{83}NO_{14}$	958	3	14	4.5	9	205	3	1810
Fedratinib	16722836	$C_{27}H_{36}N_6O_3S$	525	3	9	4.9	11	117	4	787
Fostamatinib	11671467	$C_{23}H_{26}FN_6O_9P$	580	4	15	1.7	10	187	4	904
Gefitinib	123631	$C_{22}H_{24}ClFN_4O_3$	447	1	8	4.5	8	68.7	4	545
Gilteritinib	49803313	$C_{29}H_{44}N_8O_3$	552	3	10	3.0	9	121	5	785
Ibrutinib	24821094	$C_{25}H_{24}N_6O_2$	441	1	6	3.1	5	99.2	5	678
Imatinib	5291	$C_{29}H_{31}N_7O$	494	2	7	4.2	7	86.3	5	706
Lapatinib	208908	$C_{29}H_{26}ClN_4O_4S$	580	2	9	5.0	11	115	5	898
Larotrectinib	46188928	$C_{21}H_{22}F_2N_6O_2$	428	2	7	2.6	3	86	5	659
Lenvatinib	9823820	$C_{21}H_{19}ClN_4O_4$	427	3	5	3.6	6	116	4	634
Lorlatinib	71731823	$C_{21}H_{19}FN_6O_2$	406	1	7	2.0	0	110	3	700
Midostaurin	9829523	$C_{35}H_{30}N_4O_7$	571	1	4	5.3	3	77.7	5	1140
Neratinib	9915743	$C_{30}H_{29}ClN_6O_3$	557	2	8	5.1	11	112	4	881
Netarsudil	66599893	$C_{28}H_{27}N_3O_3$	454	2	5	4.2	8	94.3	4	678
Nilotinib	644241	$C_{28}H_{22}F_3N_7O$	530	2	9	5.0	6	97.6	5	817
Nintedanib	135423438	$C_{31}H_{33}N_5O_4$	540	2	7	3.9	8	102	5	947
Osimertinib	71496458	$C_{28}H_{33}N_7O_2$	500	2	7	3.4	10	87.6	4	752
Palbociclib	5330286	$C_{24}H_{29}N_7O_2$	448	2	8	0.3	5	103	5	775
Pazopanib	10113978	$C_{21}H_{23}N_7O_2S$	438	2	8	3.8	5	127	4	717
Pemigatinib	86705659	$C_{24}H_{27}F_2N_5O_4$	487	2	7	3.4	6	88.4	5	731
Pexidartinib	25151352	$C_{20}H_{15}ClF_3N_5$	417	2	7	4.5	5	66.5	4	537
Ponatinib	24826799	$C_{29}H_{27}F_3N_6O$	533	1	8	4.7	6	65.8	5	910
Pralsetinib	129073603	$C_{27}H_{32}FN_9O_2$	534	3	9	3.5	8	136	5	816
R406	11213558	$C_{22}H_{23}FN_6O_5$	470	3	11	3.1	7	129	4	691
Regorafenib	11167602	$C_{21}H_{15}ClF_4N_4O_3$	483	3	8	4.8	5	92.4	3	686
Ribociclib	44631912	$C_{23}H_{30}N_8O$	435	2	7	2.6	5	91.2	5	636
Ripretinib	71584930	$C_{24}H_{21}BrFN_5O_2$	510	3	5	4.6	5	86.4	4	746
Ruxolitinib	25126798	$C_{17}N_{18}N_6$	306	1	4	2.0	4	83.2	4	453
Selpercatinib	134436906	$C_{29}H_{31}N_7O_3$	526	1	9	3.0	8	112	6	637
Selumetinib	10127622	$C_{17}H_{15}BrClF_4O_3$	458	3	6	3.0	6	88.4	3	523
Sirolimus	5284616	$C_{51}H_{79}NO_{13}$	914	3	13	4.5	6	195	3	1760
Sorafenib	216239	$C_{21}H_{16}ClF_3N_4O_3$	465	3	7	3.2	5	92.4	3	646
Sunitinib	5329102	$C_{22}H_{27}FN_4O_2$	398	3	4	3.2	7	77.2	3	636
Temsirolimus	6918289	$C_{56}H_{87}NO_{16}$	1029	4	16	4.3	11	242	3	2010
Tofacitinib	9926791	$C_{16}H_{20}N_6O$	312	1	5	1.0	3	88.9	3	488
Trametinib	11707110	$C_{26}H_{23}FlN_5O_4$	615	2	6	2.8	5	102	4	1090
Tucatinib	51039094	$C_{26}H_{24}N_8O_2$	481	2	8	4.4	6	111	6	796
Upadacitinib	58557659	$C_{17}H_{19}F_3N_6O$	380	2	6	0.96	3	78.3	4	561
Vandetanib	3081361	$C_{22}H_{24}BrFN_4O_2$	475	1	7	5.3	6	59.5	4	539
Vemurafenib	42611257	$C_{23}H_{18}ClF_2N_3O_3S$	490	2	7	4.9	7	100	4	790
Zanubrutinib	135565884	$C_{27}H_{27}N_5O_3$	472	2	5	2.7	6	103	5	756

[a] All data from NIH PubChem except for cLogP (the calculated Log_{10} of the partition coefficient, which was computed using MedChem Designer™, version 2.0, Simulationsplus, Inc. Lancaster, CA 93534). Drugs previously not reviewed (Refs. [9,10]) are given in **bold** type.
[b] No. of hydrogen bond donors.
[c] No. of hydrogen bond acceptors.
[d] Calculated Log_{10} of the partition coefficient.
[e] (PSA) Polar surface area.
[f] Values obtained from https://pubchem.ncbi.nlm.nih.gov/.

Table 8
Lipophilic efficiency (LipE) and ligand efficiency (LE) values and primary targets of FDA-approved drugs [g].

Drug	Target & kinase family [a]	K_i (nM) [b]	pK_i	cLogP [c]	LipE [d]	N [e]	LE [f]
Abemaciclib	CDK4, S/T	0.6	9.22	5.2	4.02	37	0.351
Acalbrutinib	BTK, NRY	3.1	8.51	1.1	7.41	35	0.343
Afatinib	EGFR, RY	0.5	9.33	4.0	5.33	34	0.387
Alectinib	ALK, RY	1.9	8.72	4.7	4.02	36	0.342
Avapritinib	PDGFRα, RY	0.18	9.7	2.7	7.0	37	0.369
Axitinib	VEGFR2, RY	0.25	9.6	3.8	5.80	28	0.483
Baricitinib	JAK2, NRY	7	8.15	0.3	7.85	26	0.442
Binimetinib	MEK1, DS	12	7.92	2.6	5.3	27	0.414
Bosutinib	BCR-Abl, NRY	20	7.7	5.0	2.70	36	0.302
Brigatinib	ALK, RY	0.398	9.4	5.2	4.20	40	0.331
Cabozantinib	RET, RY	5	8.3	4.5	3.80	37	0.390
Capmatinib	MET, RY	0.13	9.89	3.18	6.71	31	0.449
Ceritinib	ALK, RY	0.2	9.7	6.0	3.70	38	0.360
Cobimetinib	MEK1, DS	0.79	9.1	5.1	4.00	30	0.427
Crizotinib	ALK, RY	0.63	9.2	4.4	4.80	30	0.432
Dabrafenib	B-Raf, S/T	0.4	9.4	4.5	4.90	35	0.379
Dacomitinib	EGFR, RY	2.0	8.7	4.8	3.90	33	0.372
Dasatinib	BCR-Abl, NRY	0.16	9.8	3.0	6.80	33	0.419
Encorafenib	B-Raf, S/T	0.30	9.52	3.1	6.42	36	0.373
Erlotinib	EGFR, RY	0.32	9.5	3.1	6.40	29	0.462
Entrectinib	TRKA, RY	1	9.0	5.5	3.5	41	0.295
Erdafitinib	FGFR1, RY	2	8.7	4.6	4.1	33	0.372
Everolimus	FKBP12/mTOR, S/T	?	?	4.5	?	68	?
Fedratinib	JAK2, NRY	6	8.22	4.4	3.12	37	0.313
Fostamatinib	Syk, RY	17	7.77	1.7	6.07	40	0.274
Gefitinib	EGFR, RY	0.5	9.3	4.5	4.80	31	0.432
Gilteritinib	Flt3, RY	0.41	9.39	3.0	6.39	40	0.331
Ibrutinib	BTK, NRY	?	?	3.1	?	33	?
Imatinib	BCR-Abl, NRY	1	9.0	4.2	4.80	37	0.433
Lapatinib	EGFR, RY	1	9.0	5.0	4.00	40	0.325
Larotrectinib	TRK, RY	9.7	8.01	2.6	5.41	31	0.364
Lenvatinib	VEGFR2, RY	3.98	8.4	3.6	4.80	30	0.395
Lorlatinib	ALK, RY	9	8.05	2.0	6.05	30	0.378
Midostaurin	Flt3, RY	37	7.43	5.3	2.13	43	0.278
Neratinib	ErbB2/HER2, RY	59	7.23	5.1	2.13	40	0.255
Netarsudil	ROCK1/2, S/T	1	9	4.2	4.8	34	0.373
Nilotinib	BCR-Abl, NRY	12.5	7.9	5.0	2.90	39	0.286
Nintedanib	FGFR, RY	39.8	7.4	3.9	3.50	40	0.261
Osimertinib	EGFR, RY	7	8.15	3.4	4.75	37	0.311
Palbociclib	CDK4, S/T	10	8	0.3	7.70	33	0.342
Pazopanib	VEGFR2, RY	30	7.52	3.8	3.72	31	0.342
Pemigatinib	FGFR, RY	0.5	9.3	3.4	5.9	35	0.374
Pexidartinib	CSF1R, RY	13	7.89	4.5	3.4	29	0.384
Pralsetinib	RET	0.5	9.3	3.5	5.8	39	0.336
Ponatinib	BCR-Abl, NRY	1	9	4.7	4.30	39	0.326
Regorafenib	VEGFR2, RY	4.2	8.4	4.8	3.6	33	0.359
Ribociclib	CDK4, S/T	10	8	2.6	5.40	32	0.353
Ripretinib	RET, RY	3	8.52	4.64	3.88	33	0.364
Ruxolitinib	JAK1, NRY	1.2	8.92	2.0	7.92	23	0.608
Selpercatinib	RET, RY	1	9	3.0	6	39	0.325
Selumetinib	MEK1, DS	14	7.85	2.96	4.89	27	0.331
Sirolimus	FKBP12/mTOR, S/T	?	?	4.5	?	65	?
Sorafenib	VEGFR1, RY	15.8	7.8	3.2	6.60	32	0.432
Sunitinib	VEGFR2, RY	3.98	8.4	3.2	5.20	29	0.408
Temsirolimus	FKBP12/mTOR, S/T	?	?	4.3	?	73	?
Tofacitinib	JAK1, NRY	0.79	9.1	1.0	8.50	23	0.582
Trametinib	MEK1, DS	3.4	8.47	2.8	6.00	37	0.345
Tucatinib	ErbB2/HER2, RY	8	8.1	3.18	4.92	36	0.317
Upadacitinib	JAK1, NRY	43	7.37	0.96	6.41	27	0.385
Vandetanib	RET, RY	50	7.3	5.3	2.00	30	0.343
Vemurafenib	B-Raf, S/T	3.98	8.4	4.9	3.50	33	0.359
Zanubrutinib	BTK, NRY	0.3	9.52	2.7	6.82	35	0.384

[a] NRY, non-receptor protein-tyrosine kinase; RY, receptor protein-tyrosine kinase; S/T, protein-serine/threonine kinase; DS; dual specificity protein kinase (catalyzes protein-tyrosine/threonine/serine phosphorylation but evolutionarily in the protein-serine/threonine kinase family).
[b] Representative values obtained from www.ebi.ac.ug/chembl/ and from klifs.net.
[c] Calculated value of the partition coefficient using MedChem Designer™ version 2.0 Simulationsplus, Inc. Lancaster CA 93534, USA.
[d] LipE = $p\mathrm{IC}_{50}$ – cLogP, where cLogP is the calculated logarithm of the partition coefficient that was obtained using MedChem Designer™.
[e] N, Number of heavy atoms.
[f] LE = – 2.303 RT Log_{10} K_{eq}/N where N is the number of heavy (non-hydrogen) atoms in the drug.
[g] Drugs previously not reviewed (Refs. [9,10]) are given in **bold** type.

those that are not for a large series of substances in rats [125]. These investigators found that compounds with polar surface area values less than or equal to 140 $Å^2$ are orally effective. The polar surface area represents the sum of the surface over all polar atoms, primarily oxygen and nitrogen, but also including any linked hydrogen atoms. With the exceptions of six drugs (dabrafenib, encorafenib, fostamatinib, and the three macrolides), the other 56 agents have a polar surface area less than 140 $Å^2$; the average value is 103 with a range from 59.5 (vandetanib) to 242 (temsirolimus) (Table 8). Moreover, Veber et al. concluded that the optimal number of rotatable bonds should be 10 or less. This property reflects molecular flexibility (degrees of freedom) and is believed to control passive membrane permeation. Moreover, the number of degrees of freedom correlates with the entropy change associated with ligand binding and determines in part the extent of drug binding with its targets. With the exceptions of the four drugs with 11 rotatable bonds (neratinib, erlotinib, lapatinib and temsirolimus), the other drugs have 10 or fewer of these bonds. The average value is 6.5 and the number of rotatable bonds ranges from 0 (lorlatinib) to 11. Moreover, Oprea found that the number of rings in most orally approved drugs is three or greater [126]. All of the approved small molecule protein kinase inhibitors have three or more rings with an average value of 4.26 and a range from three to six. All of the FDA-approved drugs listed are orally effective with the exceptions of temsirolimus (which is given intravenously) and netarsudil (an eye drop).

The molecular complexity of a drug is based upon its elementary composition, its structural features, and any symmetry elements. The complexity is calculated using the Bertz/Hendrickson/Ihlenfelt algorithm [127,128]. It is based upon the number and identity of the constituent atoms, the nature of the chemical bonds, and the bonding pattern. The molecular complexity ranges from 0 for simple ions to several thousand for complex natural products. Intuitively, larger chemicals generally possess a higher molecular complexity value than smaller ones. In contrast, molecules containing few distinct elements and those that are highly symmetrical are characterized by a lower molecular complexity value. The molecular complexity values for the drugs in this review were obtained from PubChem (https://pubchem.ncbi.nlm.nih.gov/). For all of the FDA-approved drugs, the mean complexity value is 776 with a range from 453 (ruxolitinib) to 2010 (temsirolimus). As expected, the large macrolide medicinals exhibit the greatest molecular complexity values. There are no optimal or recommended molecular complexity values for orally effective drugs; however, this property may be helpful in determining the ease or difficulty of drug synthesis, an important consideration in the commercial production of pharmaceutical agents.

7. Epilogue and perspective

Although considerable progress has been made in the discovery and development of small molecule protein kinase inhibitors since the FDA-approval of imatinib 20 years ago, this discipline is still in its early stages. Most of the FDA- approved therapeutics are directed toward the treatment of a variety of cancers and others are directed against inflammatory diseases [9,10,110,129,130]. Because of the genetic instability of malignant cells, resistance to protein kinase therapeutics occurs on a regular and nearly universal basis. Such resistance has led to the discovery and development of second, third, and later generation antagonists that target the same enzyme and disease. Furthermore, acquired drug resistance is oftentimes due to gatekeeper mutations in the target protein kinase [3]. For example, the T790 M gatekeeper mutation in EGFR is the third most frequently observed protein kinase mutation and this mutation is responsible for about half of all instances of acquired EGFR inhibitor resistance. Although inflammatory processes per se are not characterized by genetic instability, it is unclear whether acquired resistance arises during the treatment of inflammatory disorders.

Avapritinib is used for the treatment of GIST with *PDGFRA* exon 18 mutations; other drugs have been approved for GIST (imatinib, sunitinib), but targeting the exon 18 mutations is novel. Ripretinib is another drug that targets Kit and PDGFRα and is a fourth-generation drug used for the treatment of GIST. Pralsetinib and selpercatinib are two new drugs that target RET fusion proteins and are used for the treatment of RET-fusion NSCLC, medullary thyroid cancer, and differentiated thyroid cancers. These join lenvatinib and sorafenib as drugs approved for the treatment of differentiated thyroid cancers and cabozantinib and vandetanib for the treatment of differentiated thyroid carcinomas. Capmatinib is approved for the treatment of NSCLC with MET exon 18 skipping; other drugs have been approved for NSCLC, but targeting exon 14 skipping is an original application. Pemigatinib is a FGFR2 inhibitor, but its use in the treatment of advanced cholangiocarcinomas with FGFR2 fusion proteins represents another targeted disease. Erdafitinib is a FGFR1/2/3/4 inhibitor approved for the treatment of urothelial urinary bladder cancers and nintedanib is a FGFR1/2/3 inhibitor that is used for the treatment of idiopathic pulmonary fibrosis.

Selumetinib is a dual specificity MEK1/2 inhibitor that is approved for the treatment of neurofibromatosis type I. Other MEK1/2 inhibitors include binimetinib, cobimetinib, and trametinib and these are used for the treatment of $BRAF^{V600E}$ melanomas. However, selumetinib is a medicine targeting a different disease. Tucatinib is an ErbB2/HER2 antagonist that is approved for the treatment of HER2-positive breast cancer. Capmatinib and neratinib are ErbB2/HER2 antagonists and palbociclib is a CDK4/6 antagonist, all of which are approved for the treatment of HER2-positive breast cancers. Upadacitinib joins baricitinib and tofacitinib as a JAK antagonist that is approved for the treatment of rheumatoid arthritis. Furthermore, zanubrutinib joins acalabrutinib and ibrutinib as targeted covalent inhibitors of BTK that are approved for the treatment of mantle cell lymphomas. Thus, we see that recent approvals covered herein are both later generational drugs that are directed against previous protein kinase targets as well as agents that are directed against previously untargeted diseases.

Owing to the 244 protein kinases that map to cancer amplicons or disease loci [6], it is anticipated that a substantial increase in the number of drugs inhibiting different protein kinases will be approved for the treatment of many more illnesses [131–133]. The addition of new protein kinases to the therapeutic armamentarium will require the identification of the signaling pathways that participate in the pathogenesis of currently untargeted illnesses. As the field matures during the next decades, it is certain that protein kinase inhibitors with new scaffolds, chemotypes, and pharmacophores will be formulated. There are only three FDA-approved type III allosteric inhibitors (binimetinib, cobimetinib, and trametinib) and these block the action of MEK1/2. It is expected that additional allosteric inhibitors will be developed that target different enzymes that are part of various protein kinase-regulated signal transduction modules. Moreover, it is likely that new irreversible inhibitors that target protein kinases with –SH groups near the ATP-binding site will be forthcoming.

Declaration of Competing Interest

The author is unaware of any affiliations, memberships, or financial holdings that might be perceived as affecting the objectivity of this review.

Acknowledgments

The author thanks Dr Albert J. Kooistra for providing the template depicted in Fig. 5 and the PDF IDs for several drug-enzyme complexes listed in Table 6. I thank Laura M. Roskoski for providing editorial and bibliographic assistance. I also thank Jasper Martinsek and Josie Rudnicki for their help in preparing the figures and W.S. Sheppard and Pasha Brezina for their help in structural analyses. The colored figures in this paper were evaluated to ensure that their perception was accurately conveyed to colorblind readers [134].

Appendix A. Supplementary data

Supplementary material related to this article can be found, in the online version, at doi:https://doi.org/10.1016/j.phrs.2021.105463.

References

[1] R. Roskoski Jr., A historical overview of protein kinases and their targeted small molecule inhibitors, Pharmacol. Res. 100 (2015) 1–23.
[2] P. Cohen, Protein kinases – the major drug targets of the twenty-first century? Nat. Rev. Drug Discov. 1 (2002) 309–315.
[3] G.K. Kanev, C. de Graaf, I.J.P. de Esch, R. Leurs, T. Würdinger, B.A. Westerman, et al., The landscape of atypical and eukaryotic protein kinases, Trends Pharmacol. Sci. 40 (2019) 818–832.
[4] C. Bournez, F. Carles, G. Peyrat, S. Aci-Sèche, S. Bourg, C. Meyer, et al., Comparative assessment of protein kinase inhibitors in public databases and in PKIDB, Molecules 25 (14) (2020) 3226, https://doi.org/10.3390/molecules25143226.
[5] P.M. Fischer, Approved and experimental small-molecule oncology kinase inhibitor drugs: a mid-2016 overview, Med. Res. Rev. 37 (2017) 314–367.
[6] G. Manning, D.B. Whyte, R. Martinez, T. Hunter, S. Sudarsanam, The protein kinase complement of the human genome, Science 298 (2002) 1912–1934.
[7] S.H. Myers, V.G. Brunton, A. Unciti-Broceta, AXL inhibitors in cancer: a medicinal chemistry perspective, J. Med. Chem. 59 (2016) 3593–3608.
[8] B.L. Roth, D.J. Sheffler, W.K. Kroeze, Magic shotguns versus magic bullets: selectively non-selective drugs for mood disorders and schizophrenia, Nat. Rev. Drug Discov. 3 (2004) 353–359.
[9] R. Roskoski Jr., Properties of FDA-approved small molecule protein kinase inhibitors, Pharmacol. Res. 144 (2019) 19–50.
[10] R. Roskoski Jr., Properties of FDA-approved small molecule protein kinase inhibitors: a 2020 update, Pharmacol. Res. 152 (2020) 104609.
[11] R. Roskoski Jr., Orally effective FDA-approved protein kinase targeted covalent inhibitors (TCIs), Pharmacol. Res. (2021), https://doi.org/10.1016/j.phrs.2021.105422.
[12] D.R. Knighton, J.H. Zheng, L.F. Ten Eyck, V.A. Ashford, N.H. Xuong, S.S. Taylor, et al., Crystal structure of the catalytic subunit of cyclic adenosine monophosphate-dependent protein kinase, Science 253 (1991) 407–414.
[13] S.S. Taylor, A.P. Kornev, Protein kinases: evolution of dynamic regulatory proteins, Trends Biochem. Sci. 36 (2011) 65–77.
[14] A.P. Kornev, S.S. Taylor, Dynamics-driven allostery in protein kinases, Trends Biochem. Sci. 40 (2015) 628–647.
[15] R. Roskoski Jr., Cyclin-dependent protein serine/threonine kinase inhibitors as anticancer drugs, Pharmacol. Res. 139 (2019) 471–488.
[16] S.K. Hanks, T. Hunter, Protein kinases 6. The eukaryotic protein kinase superfamily: kinase (catalytic) domain structure and classification, FASEB J. 9 (1995) 576–596.
[17] Madhusudan, E.A. Trafny, N.H. Xuong, J.A. Adams, L.F. Ten Eyck, S.S. Taylor, et al., cAMP-dependent protein kinase: crystallographic insights into substrate recognition and phosphotransfer, Protein Sci. 3 (1994) 176–187.
[18] J. Zhou, J.A. Adams, Participation of ADP dissociation in the rate-determining step in cAMP-dependent protein kinase, Biochemistry 36 (1997) 15733–15738.
[19] P.A. Schwartz, B.W. Murray, Protein kinase biochemistry and drug discovery, Bioorg. Chem. 39 (2011) 192–210.
[20] A.P. Kornev, S.S. Taylor, Defining the conserved internal architecture of a protein kinase, Biochim. Biophys. Acta 1804 (2010) 440–444.
[21] A.P. Kornev, N.M. Haste, S.S. Taylor, L.F. Eyck, Surface comparison of active and inactive protein kinases identifies a conserved activation mechanism, Proc Natl Acad Sci U S A 103 (2006) 17783–17788.
[22] A.P. Kornev, S.S. Taylor, L.F. Ten Eyck, A helix scaffold for the assembly of active protein kinases, Proc Natl Acad Sci U S A 105 (2008) 14377–14382.
[23] H.S. Meharena, P. Chang, M.M. Keshwani, K. Oruganty, A.K. Nene, N. Kannan, et al., Deciphering the structural basis of eukaryotic protein kinase regulation, PLoS Biol. 11 (2013), e1001690.
[24] R. Roskoski Jr., Classification of small molecule protein kinase inhibitors based upon the structures of their drug-enzyme complexes, Pharmacol. Res. 103 (2016) 26–48.
[25] R. Roskoski Jr., Anaplastic lymphoma kinase (ALK): structure, oncogenic activation, and pharmacological inhibition, Pharmacol. Res. 68 (2013) 68–94.
[26] R. Roskoski Jr., Anaplastic lymphoma kinase (ALK) inhibitors in the treatment of ALK-driven lung cancers, Pharmacol. Res. 117 (2017) 343–356.
[27] R. Roskoski Jr., The preclinical profile of crizotinib in the treatment of non-small cell lung cancer and other neoplastic disorders, Expert Opin Drug Dis. 8 (2013) 1165–1179.
[28] R. Roskoski Jr., The ErbB/HER family of protein-tyrosine kinases and cancer, Pharmacol. Res. 79 (2014) 34–74.
[29] R. Roskoski Jr., ErbB/HER protein-tyrosine kinases: structure and small molecule inhibitors, Pharmacol. Res. 87 (2014) 42–59.
[30] R. Roskoski Jr., Small molecule inhibitors targeting the EGFR/ErbB family of protein-tyrosine kinases in human cancers, Pharmacol. Res. 139 (2019) 395–411.
[31] R. Roskoski Jr., The role of fibroblast growth factor receptor (FGFR) protein-tyrosine kinase inhibitors in the treatment of cancers including those of the urinary bladder, Pharmacol. Res. 151 (2020), 104567.
[32] R. Roskoski Jr., The role of small molecule kit protein-tyrosine kinase inhibitors in the treatment of neoplastic disorders, Pharmacol. Res. 133 (2018) 35–52.
[33] R. Roskoski Jr., The role of small molecule platelet-derived growth factor receptor (PDGFR) inhibitors in the treatment of neoplastic disorders, Pharmacol. Res. 129 (2018) 65–83.
[34] R. Roskoski Jr., A. Sadeghi-Nejad, Role of RET protein-tyrosine kinase inhibitors in the treatment RET-driven thyroid and lung cancers, Pharmacol. Res. 128 (2018) 1–17.
[35] R. Roskoski Jr., Vascular endothelial growth factor (VEGF) and VEGF receptor inhibitors in the treatment of renal cell carcinomas, Pharmacol. Res. 120 (2017) 116–132.
[36] R. Roskoski Jr., ROS1 protein-tyrosine kinase inhibitors in the treatment of ROS1 fusion protein-driven non-small cell lung cancers, Pharmacol. Res. 121 (2017) 202–212.
[37] R. Roskoski Jr., Ibrutinib inhibition of Bruton protein-tyrosine kinase (BTK) in the treatment of B cell neoplasms, Pharmacol. Res. 113 (2016) 395–408.
[38] R. Roskoski Jr., Src protein-tyrosine kinase structure, mechanism, and small molecule inhibitors, Pharmacol. Res. 94 (2015) 9–25.
[39] M.C. Frame, R. Roskoski Jr., Src family tyrosine kinases. Reference Module in Life Sciences, Elsevier, Amsterdam, 2017, pp. 1–11, https://doi.org/10.1016/B978-0-12-809633-8.07199-5.
[40] R. Roskoski Jr., Janus kinase (JAK) inhibitors in the treatment of inflammatory and neoplastic diseases, Pharmacol. Res. 111 (2016) 784–803.
[41] R. Roskoski Jr., Allosteric MEK1/2 inhibitors including cobimetanib and trametinib in the treatment of cutaneous melanomas, Pharmacol. Res. 117 (2017) 20–31.
[42] R. Roskoski Jr., ERK1/2 MAP kinases: structure, function, and regulation, Pharmacol. Res. 66 (2012) 105–143.
[43] R. Roskoski Jr., Targeting ERK1/2 protein-serine/threonine kinases in human cancers, Pharmacol. Res. 142 (2019) 151–168.
[44] R. Roskoski Jr., Cyclin-dependent protein kinase inhibitors including palbociclib as anticancer drugs, Pharmacol. Res. 111 (2016) 784–803.
[45] R. Roskoski Jr., Targeting oncogenic Raf protein-serine/threonine kinases in human cancers, Pharmacol. Res. 135 (2018) 239–258.
[46] R. Roskoski Jr., RAF protein-serine/threonine kinases: structure and regulation, Biochem. Biophys. Res. Commun. 399 (2010) 313–317.
[47] Y. Liu, K. Shah, F. Yang, L. Witucki, K.M. Shokat, A molecular gate which controls unnatural ATP analogue recognition by the tyrosine kinase v-Src, Bioorg. Med. Chem. 6 (1998) 1219–1226.
[48] A.C. Dar, K.M. Shokat, The evolution of protein kinase inhibitors from antagonists to agonists of cellular signaling, Annu. Rev. Biochem. 80 (2011) 769–795.
[49] P.M. Ung, R. Rahman, A. Schlessinger, Redefining the protein kinase conformational space with machine learning, Cell Chem. Biol. 25 (2018), 916-24.e2.
[50] R. Hu, H. Xu, P. Jia, Z. Zhao, KinaseMD: kinase mutations and drug response database, Nucleic Acids Res. 49 (D1) (2021) D552–61.
[51] F. Zuccotto, E. Ardini, E. Casale, M. Angiolini, Through the "gatekeeper door": exploiting the active kinase conformation, J. Med. Chem. 53 (2010) 2691–2694.
[52] L.K. Gavrin, E. Saiah, Approaches to discover non-ATP site inhibitors, Med. Chem. Res. 4 (2013) 41.
[53] V. Lamba, I. Ghosh, New directions in targeting protein kinases: focusing upon true allosteric and bivalent inhibitors, Curr. Pharm. Des. 18 (2012) 2936–2945.
[54] J.J. Liao, Molecular recognition of protein kinase binding pockets for design of potent and selective kinase inhibitors, J. Med. Chem. 50 (2007) 409–424.
[55] O.P. van Linden, A.J. Kooistra, R. Leurs, I.J. de Esch, C. de Graaf, KLIFS: a knowledge-based structural database to navigate kinase-ligand interaction space, J. Med. Chem. 57 (2014) 249–277.
[56] G.K. Kanev, C. de Graaf, B.A. Westerman, I.J.P. de Esch, A.J. Kooistra, KLIFS: an overhaul after the first 5 years of supporting kinase research, Nucleic Acids Res. (2020), https://doi.org/10.1093/nar/gkaa895 gkaa895.
[57] B. Wienen-Schmidt, D. Schmidt, H.D. Gerber, A. Heine, H. Gohlke, G. Klebe, Surprising non-additivity of methyl groups in drug-kinase interaction, ACS Chem. Biol. 14 (December (12)) (2019) 2585–2594.
[58] D. Bajusz, G.G. Ferenczy, G.M. Keserá, Structure-based virtual screening approaches in kinase-directed drug discovery, Curr. Top. Med. Chem. 17 (2017) 2235–2259.
[59] P. Wu, T.E. Nielsen, M.H. Clausen, FDA-approved small-molecule kinase inhibitors, Trends Pharmacol. Sci. 36 (2015) 422–439.
[60] L. Huang, S. Jiang, Y. Shi, Tyrosine kinase inhibitors for solid tumors in the past 20 years (2001-2020), J. Hematol. Oncol. 13 (2020) 143.
[61] V. Subbiah, T. Shen, S.S. Terzyan, X. Liu, X. Hu, K.P. Patel, et al., Structural basis of acquired resistance to selpercatinib and pralsetinib mediated by non-gatekeeper RET mutations, Ann. Oncol. (2020), https://doi.org/10.1016/j.annonc.2020.10.599. S0923-7534(20)43127-43128.
[62] A. Markham, Pralsetinib: first approval, Drugs 80 (2020) 1865–1870.
[63] K.M. Wright, FDA approves pralsetinib for treatment of adults with metastatic RET fusion-positive NSCLC, Oncology (Williston Park) 34 (2020) 406.
[64] M.C. Heinrich, C.L. Corless, A. Duensing, L. McGreevey, C.J. Chen, N. Joseph, et al., *PDGFRA* activating mutations in gastrointestinal stromal tumors, Science 299 (2003) 708–710.
[65] C. Serrano, S. George, Recent advances in the treatment of gastrointestinal stromal tumors, Ther. Adv. Med. Oncol. 6 (2014) 115–127.
[66] C.L. Corless, C.M. Barnett, M.C. Heinrich, Gastrointestinal stromal tumours: origin and molecular oncology, Nat. Rev. Cancer 11 (2011) 865–878.
[67] C.H. Heldin, J. Lennartsson, B. Westermark, Involvement of platelet-derived growth factor ligands and receptors in tumorigenesis, J. Intern. Med. 283 (2018) 16–44.

[68] C. Bahlawane, R. Eulenfeld, M.Y. Wiesinger, J. Wang, A. Muller, A. Girod, et al., Constitutive activation of oncogenic PDGFRα-mutant proteins occurring in GIST patients induces receptor mislocalisation and alters PDGFRα signalling characteristics, Cell Commun. Signal 13 (2015) 21.
[69] M.C. Heinrich, C.L. Corless, G.D. Demetri, C.D. Blanke, M. von Mehren, H. Joensuu, et al., Kinase mutations and imatinib response in patients with metastatic gastrointestinal stromal tumor, J. Clin. Oncol. 21 (2003) 4342–4349.
[70] M.C. Heinrich, R.G. Maki, C.L. Corless, C.R. Antonescu, A. Harlow, D. Griffith, et al., Primary and secondary kinase genotypes correlate with the biological and clinical activity of sunitinib in imatinib-resistant gastrointestinal stromal tumor, J. Clin. Oncol. 26 (2008) 5352–5359.
[71] P. Reichardt, G.D. Demetri, H. Gelderblom, P. Rutkowski, S.A. Im, S. Gupta, et al., Correlation of *KIT* and *PDGFRA* mutational status with clinical benefit in patients with gastrointestinal stromal tumor treated with sunitinib in a worldwide treatment-use trial, BMC Cancer 16 (2016) 22, https://doi.org/10.1186/s12885-016-2051–5.
[72] B.D. Smith, M.D. Kaufman, W.P. Lu, A. Gupta, C.B. Leary, S.C. Wise, et al., Ripretinib (DCC-2618) is a switch control kinase inhibitor of a broad spectrum of oncogenic and drug-resistant KIT and PDGFRA variants, Cancer Cell 35 (2019) 738–751, e9.
[73] J. Nemunaitis, S. Bauer, J.Y. Blay, K. Choucair, H. Gelderblom, S. George, et al., Intrigue: phase III study of ripretinib versus sunitinib in advanced gastrointestinal stromal tumor after imatinib, Future Oncol. 16 (2020) 4251–4264.
[74] M. Das, Zanubrutinib in B-cell malignancies, Lancet Oncol. 20 (2019) e470.
[75] Y.Y. Syed, Zanubrutinib: first approval, Drugs 80 (2020) 91–97.
[76] H.C. Kluin-Nelemans, E. Hoster, O. Hermine, J. Walewski, M. Trneny, C. H. Geisler, et al., Treatment of older patients with mantle-cell lymphoma, N. Engl. J. Med. 367 (2012) 520–531.
[77] Y. Guo, Y. Liu, N. Hu, D. Yu, C. Zhou, G. Shi, et al., Discovery of zanubrutinib (BGB-3111), a novel, potent, and selective covalent inhibitor of Bruton's tyrosine kinase, J. Med. Chem. 62 (2019) 7923–7940.
[78] M. Bergoug, M. Doudeau, F. Godin, C. Mosrin, B. Vallée, H. Bénédetti, Neurofibromin structure, functions and regulation, Cells 9 (2020) 2365.
[79] R.E. Strowd 3rd., Available therapies for patients with neurofibromatosis-related nervous system tumors, Curr. Treat. Options Oncol. 21 (2020) 81.
[80] A.M. Gross, E. Dombi, B.C. Widemann, Current status of MEK inhibitors in the treatment of plexiform neurofibromas, Childs Nerv. Syst. 36 (2020) 2443–2452.
[81] K.D. Robarge, W. Lee, C. Eigenbrot, M. Ultsch, C. Wiesmann, R. Heald, et al., Structure based design of novel 6,5 heterobicyclic mitogen-activated protein kinase kinase (MEK) inhibitors leading to the discovery of imidazo[1,5-a] pyrazine G-479, Bioorg. Med. Chem. Lett. 24 (2014) 4714–4723.
[82] C.P. Joseph, S.N. Abaricia, M.A. Angelis, K. Polson, R.L. Jones, Y.K. Kang, et al., Optimal Avapritinib treatment strategies for patients with metastatic or unresectable gastrointestinal stromal tumors, Oncologist (2020), https://doi.org/10.1002/onco.13632.
[83] J. Florindez, J. Trent, Low frequency of mutation testing in the United States: an analysis of 3866 GIST patients, Am. J. Clin. Oncol. 43 (2020) 270–278.
[84] A.K. Gardino, E.K. Evans, J.L. Kim, N. Brooijmans, B.L. Hodous, B. Wolf, et al., Targeting kinases with precision, Mol. Cell. Oncol. 5 (2018), e1435183.
[85] S. Dhillon, Capmatinib: first approval, Drugs 80 (2020) 1125–1131.
[86] C.S. Cooper, M. Park, D.G. Blair, M.A. Tainsky, K. Huebner, C.M. Croce, G. F. Vande Woude, Molecular cloning of a new transforming gene from a chemically transformed human cell line, Nature 311 (1984) 29–33.
[87] L. Trusolino, A. Bertotti, P.M. Comoglio, MET signalling: principles and functions in development, organ regeneration and cancer, Nat. Rev. Mol. Cell Biol. 11 (2010) 834–848.
[88] J.J. Cui, M. Tran-Dubé, H. Shen, M. Nambu, P.P. Kung, M. Pairish, et al., Structure based drug design of crizotinib (PF-02341066), a potent and selective dual inhibitor of mesenchymal-epithelial transition factor (c-MET) kinase and anaplastic lymphoma kinase (ALK), J. Med. Chem. 54 (2011) 6342–6363.
[89] X. Liu, Q. Wang, G. Yang, C. Marando, H.K. Koblish, L.M. Hall, et al., A novel kinase inhibitor, INCB28060, blocks c-MET-dependent signaling, neoplastic activities, and cross-talk with EGFR and HER-3, Clin. Cancer Res. 17 (2011) 7127–7138.
[90] J.P. Eder, G.F. Vande Woude, S.A. Boerner, P.M. LoRusso, Novel therapeutic inhibitors of the c-Met signaling pathway in cancer, Clin. Cancer Res. 15 (2009) 2207–2214.
[91] S. Peters, A.A. Adjei, MET: a promising anticancer therapeutic target, Nat. Rev. Clin. Oncol. 9 (2012) 314–326.
[92] E. Gherardi, W. Birchmeier, C. Birchmeier, G. Vande Woude, Targeting MET in cancer: rationale and progress, Nat. Rev. Cancer 12 (2012) 89–103.
[93] J. Gao, Y. Inagaki, P. Song, X. Qu, N. Kokudo, W. Tang, Targeting c-Met as a promising strategy for the treatment of hepatocellular carcinoma, Pharmacol. Res. 65 (2012) 23–30.
[94] M.F. Di Renzo, M. Olivero, T. Martone, A. Maffe, P. Maggiora, A.D. Stefani, et al., Somatic mutations of the MET oncogene are selected during metastatic spread of human HNSC carcinomas, Oncogene 19 (2000) 1547–1555.
[95] I.M. Silverman, A. Hollebecque, L. Friboulet, S. Owens, R.C. Newton, H. Zhen, et al., Clinicogenomic analysis of FGFR2-rearranged cholangiocarcinoma identifies correlates of response and mechanisms of resistance to pemigatinib, Cancer Discov. (2020). CD-20-0766.
[96] S.M. Hoy, Pemigatinib: first approval, Drugs 80 (2020) 923–929.
[97] A. Rizzo, S. Tavolari, A.D. Ricci, G. Frega, A. Palloni, V. Relli, et al., Molecular features and targeted therapies in extrahepatic cholangiocarcinoma: promises and failures, Cancers (Basel) 12 (2020) 3256.
[98] A. Lee, Tucatinib: first approval, Drugs 80 (2020) 1033–1038.
[99] R.L. Siegel, K.D. Miller, A. Goding Sauer, S.A. Fedewa, L.F. Butterly, J. C. Anderson, et al., Colorectal cancer statistics, 2020, CA Cancer J. Clin. 70 (2020) 145–164.
[100] F. Bray, J. Ferlay, I. Soerjomataram, R.L. Siegel, L.A. Torre, A. Jemal, Global cancer statistics 2018: GLOBOCAN estimates of incidence and mortality worldwide for 36 cancers in 185 countries, CA Cancer J. Clin. (2018), https://doi.org/10.3322/caac.21492.
[101] J.L. Wittliff, Steroid-hormone receptors in breast cancer, Cancer 53 (1984) 630–643.
[102] P. Tarantino, A. Prat, J. Cortes, F. Cardoso, G. Curigliano, Third-line treatment of HER2-positive advanced breast cancer: from no standard to a Pandora's box, Biochim. Biophys. Acta Rev. Cancer 1875 (2020), 188487.
[103] A. Kulukian, P. Lee, J. Taylor, R. Rosler, P. de Vries, D. Watson, et al., Preclinical activity of HER2-selective tyrosine kinase inhibitor tucatinib as a single agent or in combination with trastuzumab or docetaxel in solid tumor models, Mol. Cancer Ther. 19 (2020) 976–987.
[104] R.K. Murthy, S. Loi, A. Okines, E. Paplomata, E. Hamilton, S.A. Hurvitz, et al., Tucatinib, trastuzumab, and capecitabine for HER2-positive metastatic breast Cancer, N. Engl. J. Med. 382 (2020) 597–609.
[105] S. Duggan, S.J. Keam, Upadacitinib: first approval, Drugs 79 (2019) 1819–1828.
[106] V. Reddy, S. Cohen, JAK inhibitors: what is new? Curr. Rheumatol. Rep. 22 (2020) 50.
[107] D.L. Scott, F. Wolfe, T.W. Huizinga, Rheumatoid arthritis, Lancet 376 (2010) 1094–1108.
[108] R.F. van Vollenhoven, R. Fleischmann, S. Cohen, E.B. Lee, J.A. García Meijide, S. Wagner, et al., Tofacitinib or adalimumab versus placebo in rheumatoid arthritis, N. Engl. J. Med. 367 (2012) 508–519.
[109] E.B. Lee, R. Fleischmann, S. Hall, B. Wilkinson, J.D. Bradley, D. Gruben, et al., Tofacitinib versus methotrexate in rheumatoid arthritis, N. Engl. J. Med. 370 (2014) 2377–2386.
[110] A.A. Zarrin, K. Bao, P. Lupardus, D. Vucic, Kinase inhibition in autoimmunity and inflammation, Nat. Rev. Drug Discov. 20 (2021) 39–63.
[111] G. Kim, J.C. Barner, K. Rascati, K. Richards, Examining time to initiation of biologic disease-modifying antirheumatic drugs and medication adherence and persistence among Texas medicaid recipients with rheumatoid arthritis, Clin. Ther. 38 (2016) 646–654.
[112] T. Dörner, V. Strand, P. Cornes, J. Gonçalves, L. Gulácsi, J. Kay, et al., The changing landscape of biosimilars in rheumatology, Ann. Rheum. Dis. 75 (2016) 974–982.
[113] A.F. Wilks, The JAK kinases: not just another kinase drug discovery target, Semin. Cell Dev. Biol. 19 (2008) 319–328.
[114] M. Kawamura, D.W. McVicar, J.A. Johnston, T.B. Blake, Y.Q. Chen, B.K. Lal, et al., Molecular cloning of L-JAK, a Janus family protein-tyrosine kinase expressed in natural killer cells and activated leukocytes, Proc Natl Acad Sci U S A 91 (1994) 6374–6378.
[115] J.J. O'Shea, D.M. Schwartz, A.V. Villarino, M. Gadina, I.B. McInnes, A. Laurence, The JAK-STAT pathway: impact on human disease and therapeutic intervention, Annu. Rev. Med. 66 (2015) 311–328.
[116] J.M. Parmentier, J. Voss, C. Graff, A. Schwartz, M. Argiriadi, M. Friedman, et al., In vitro and in vivo characterization of the JAK1 selectivity of upadacitinib (ABT-494), BMC Rheumatol 2 (2018) 23.
[117] I.B. McInnes, N.L. Byers, R.E. Higgs, J. Lee, W.L. Macias, S. Na, et al., Comparison of baricitinib, upadacitinib, and tofacitinib mediated regulation of cytokine signaling in human leukocyte subpopulations, Arthritis Res. Ther. 2 (21) (2019) 183.
[118] C.A. Lipinski, F. Lombardo, B.W. Dominy, P.J. Feeney, Experimental and computational approaches to estimate solubility and permeability in drug discovery and development settings, Adv. Drug Deliv. Rev. 46 (2001) 3–26.
[119] A.L. Hopkins, C.R. Groom, A. Alex, Ligand efficiency: a useful metric for lead selection, Drug Discov. Today 9 (2004) 430–431.
[120] G.F. Smith, Medicinal chemistry by the numbers: the physicochemistry, thermodynamics and kinetics of modern drug design, Prog. Med. Chem. 48 (2009) 1–29.
[121] P.D. Leeson, B. Springthorpe, The influence of drug-like concepts on decision-making in medicinal chemistry, Nat. Rev. Drug Discov. 6 (2007) 881–890.
[122] S. Ekins, N.K. Litterman, C.A. Lipinski, B.A. Bunin, Thermodynamic proxies to compensate for biases in drug discovery methods, Pharm. Res. 33 (2016) 194–205.
[123] A.L. Hopkins, G.M. Keserü, P.D. Leeson, D.C. Rees, C.H. Reynolds, The role of ligand efficiency metrics in drug discovery, Nat. Rev. Drug Discov. 13 (2014) 105–121.
[124] P.D. Leeson, Molecular inflation, attrition, and the rule of five, Adv. Drug Deliv. Rev. 101 (2016) 22–33.
[125] D.F. Veber, S.R. Johnson, H.Y. Cheng, B.R. Smith, K.W. Ward, K.D. Kopple, Molecular properties that influence the oral bioavailability of drug candidates, J. Med. Chem. 45 (2002) 2615–2623.
[126] T.I. Oprea, Property distribution of drug-related chemical databases, J. Comput. Aided Mol. Des. 14 (2000) 251–264.
[127] S.H. Bertz, The first general index of molecular complexity, J. Am. Chem. Soc. 1103 (1981) 3559–3601.
[128] J.B. Hendrickson, P. Huang, A.G. Toczko, Molecular complexity: a simplified formula adapted to individual atoms, J Chem Inf Compout Sci 27 (1987) 63–67.
[129] K. Bechman, M. Yates, J.B. Galloway, The new entries in the therapeutic armamentarium: the small molecule JAK inhibitors, Pharmacol. Res. 147 (2019), 104392.

[130] K. Bechman, J.B. Galloway, K.L. Winthrop, Small-molecule protein kinase inhibitors and the risk of fungal infections, Curr. Fungal Infect. Rep. (2021), https://doi.org/10.1007/s12281-019-00350-w.
[131] T.I. Oprea, C.G. Bologa, S. Brunak, A. Campbell, G.N. Gan, A. Gaulton, et al., Unexplored therapeutic opportunities in the human genome, Nat. Rev. Drug Discov. 17 (2018) 317–332.
[132] C.I. Wells, H. Al-Ali, D.M. Andrews, R.M. Asquith, A.D. Axtman, I. Dikic, et al., The kinase chemogenomic set (KCGS): an open science resource for kinase vulnerability identification, Int. J. Mol. Sci. 22 (2021) 566.
[133] J. Choo, G. Heo, C. Pothoulakis, E. Im, Posttranslational modifications as therapeutic targets for intestinal disorders, Pharmacol. Res. (2021), 105412, https://doi.org/10.1016/j.phrs.2020.105412.
[134] R. Roskoski Jr., Guidelines for preparing color figures for everyone including the colorblind, Pharmacol. Res. 119 (2017), 240–1. Erratum in: Pharmacol Res 2019; 139:569.